GRØNLANDS GEOLOGISKE UNDERSØGELSE

Bulletin No. 127

The ore minerals of the Ilímaussaq intrusion: their mode of occurrence and their conditions of formation

by

S. Karup-Møller

KØBENHAVN 1978

Grønlands Geologiske Undersøgelse

(The Geological Survey of Greenland)

Øster Voldgade 10, DK-1350 Copenhagen K

Bulletins

The ore minerals of the Ilímaussaq intrusion: their mode of occurrence and their conditions of formation

by

S. Karup-Møller

1978

Abstract

On the basis of their chemical composition, the Ilímaussaq ore minerals in pegmatites and hydro-thermal veins have been subdivided into the following four associations: I Pb-Zn-Mo, II Cu-Sb (including two subtypes: IIA Cu-Sb and IIB Cu-Sb-S), III Fe-As and IV Fe-Ni-As-Sb.

Accessory rock-forming ore minerals have been studied in heavy mineral concentrates isolated from the augite syenite and from the following agpaitic rocks: alkali granite, sodalite foyaite, naujaite, green lujavrite, medium- to coarse-grained lujavrite and black, red and white kakortokites. The ore minerals comprise sulphides (galena, sphalerite, molybdenite, pyrrhotite, troilite, marcasite, pyrite, chalcopyrite and djerfisherite), native elements (tin, lead and iron), alloys (seinäjokite [$FeSb_2$] and unnamed Sn-Cu(-Pb)phase), arsenides (westerveldite and loellingite) and one antimonide (gudmundite). Oxides of iron, titanium and chromium have been identified. Native iron, native tin, unnamed Sn-Cu(-Pb)phase, decomposed wüstite and chromite may represent contaminated material. Some of the accessory rock forming ore minerals form two additional associations: V Fe-Cu and VI Fe-Ti-O.

The accessory ore minerals in the agpaitic rocks crystallized relatively late compared to the silicate minerals. In the augite syenite the original pyrrhotite and associated chalcopyrite crystallized from an immiscible sulphide phase. Correlation between accessory rock-forming ore minerals and bulk chemical composition of the major rocks is severely limited due to the lack of chemical data.

The ore minerals in the rocks, pegmatites and veins crystallized at low sulphur and oxygen fugacities. The $\log a_{S2}$ and $\log f_{O2}$ ranges are semi-quantitatively estimated on the basis of published thermodynamic data.

Author's address:
Mineralogical Institute
Technical University of Denmark
2800 Lyngby
Denmark

CONTENTS

Fig. 1. Geological map of the Ilímaussaq intrusion (modified after Ferguson, 1964) showing sample localities mentioned in fig. 4. 1-4: Cu-Sb-(S) occurrences (Karup-Møller et al., 1977), 5-6: native lead occurrences (Karup-Møller, 1975), 7: Fe-Ni-As-Sb occurrences (Oen & Sørensen, 1964) and A-G: Fe-As occurrences (Karup-Møller & Makovicky, 1977).

INTRODUCTION

The Ilímaussaq intrusion (fig. 1), the Ivigtut cryolite deposit and the Grønne-dal-Ika carbonatite complex in South Greenland belong, together with several other syenite, nepheline syenite and granite intrusions, to the Gardar igneous province. Unusually diversified ore and silicate mineralogy characterize the Ilímaussaq intrusion and the cryolite deposit while other Gardar intrusions have not yet yielded any ore minerals of special interest.

A relatively large number of ore minerals occur in pegmatites and pneumatolytic-hydrothermal veins within the Ilímaussaq intrusion. Galena, sphalerite and molybdenite are relatively common accessory constituents. Cu-Sb minerals have been found at five localities (Karup-Møller, 1974; Karup-Møller & Makovicky, 1974; Karup-Møller et al. 1978), Fe-As minerals at several localities (Karup-Møller & Makovicky, 1977), Fe-Ni-As-Sb minerals at one locality (Oen & Sørensen, 1964) and native lead at two localities (Karup-Møller, 1975).

Examination of the heavy mineral concentrates extracted from several of the major rock types from the Ilímaussaq intrusion showed the existence of a large number of accessory ore minerals.

All the ore minerals from the Ilímaussaq intrusion have been classified according to paragenesis and chemical composition. Their conditions of formation have been discussed in relation to: (1) sulphur and oxygen fugacities, (2) age relationship between ore and silicate minerals, and (3) bulk chemical composition of host rocks versus type and ore mineral content.

GEOLOGICAL SETTING OF THE ILÍMAUSSAQ INTRUSION

The Gardar igneous province to which the Ilímaussaq intrusion belongs was emplaced into a Proterozoic (Ketilidian) basement composed dominantly of granitic material which locally contains remnants of earlier sediments and lavas. The last magmatic and regional metamorphic events in this basement occurred between 1600 and 1750 m.y. ago.

Erosion of the Ketilidian rocks and subsequent sedimentation (Igaliko arkosic sandstones) was followed during the Gardar period by extrusion of mafic lavas,

intrusion of alkaline massifs and emplacement of numerous dyke swarms. The emplacement of these rocks was controlled by WNW-ESE trending faults in a way resembling features of a modern rift valley system. Magmatism during this period appears to have reached its peak between 1250 and 1150 m.y. ago (Van Breemen & Upton, 1972).

The Gardar intrusive rocks, apart from the cryolite deposit, the Ilímaussaq intrusion and the Grønnedal-Ika complex, range in composition from calc-alkaline syenites to nepheline syenites and granites. The Gardar dykes range in composition from olivine gabbros, dolerites, syenite-trachytes, microgranites and phonolites. All the intrusions are derived from a huge deep-seated alkali basaltic Gardar magma some 250-500 km long and 50-100 km broad. This may have been layered with alkalies concentrated in the upper part thus leading to the predominance of alkaline rocks within the Gardar province (Bridgwater & Harry, 1968; Upton, 1974).

The geology and mineralogy of the Ilímaussaq intrusion has been dealt with in many publications. A complete reference list of publications up to 1967 is given by Sørensen (1967). In summary, the Ilímaussaq intrusion may be subdivided into an *older unstratified part* and a *younger stratified part* (Ussing, 1912; Sørensen, 1958, 1970; Ferguson, 1964, 1970). The stratified rocks, mainly the naujaites and the kakortokites, are cut by pegmatites and pneumatolytic veins of late magmatic origin.

The roof of the intrusion, lavas and sandstones, is known at many localities; the floor is not exposed.

The *unstratified part* of the intrusion consists of augite syenite, which forms a shell chilled against the country rocks, partly enclosing the central stratified rocks. Alkali granite and quartz syenite occur as a sheet in the topmost areas of the intrusion above the stratified rocks, but their mode of emplacement has not been solved. (fig. 1.)

The *stratified rocks* of the Ilímaussaq intrusion are nepheline syenites. They comprise in ideal section from top to bottom (thickness in brackets has been taken from Sørensen, 1958): pulaskite and heterogeneous foyaite (2–40 m), sodalite foyaite 2–150 m), naujaite (400 m), lujavrites (up to 300 m) and kakortokites (minimum 400 m). Pulaskite and heterogeneous foyaite are slightly agpaitic, the remaining rocks strongly agpaitic. A Rb-Sr whole-rock isochron has given an age of 1168±21 m.y. for the agpaitic rocks of the Ilímaussaq intrusion (Blaxland *et al.,* 1976).

The upper part of the intrusion crystallized downwards. Pulaskite and heterogeneous foyaite gradually change into sodalite foyaite. Naujaites crystallized as a result of flotation accumulation of early formed sodalite (hackmanite) which may constitute up to 70 per cent of the rocks.

Kakortokites occupy the lowermost portion of the exposed part of the intrusion and consist of a repeated three-member rock sequence. From the bottom to the

top, each sequence consists of the following rock types: (1) black arfvedsonite-rich kakortokite ($\sim$ 1.5 m), (2) red eudialyte-rich kakortokite ($\sim$ 1.5 m), and (3) white microcline-rich kakortokite ($\sim$ 10 m). (Details are given by Bohse et al., 1971).

The lujavrites occur between the earlier formed naujaites and kakortokites. They have intruded the naujaites and often contain large inclusions of these rocks. According to Ferguson (1970) and Bohse et al. (1971) the lujavrites conformably overlie the kakortokites. The two major lujavrite varieties are green aegirine-rich lujavrite and black arfvedsonite-rich lujavrite. Medium to coarse-grained lujavrite (called lujavrite MC in this paper) occurs only within the Kvanefjeld area in the northern part of the intrusion (Sørensen et al., 1969a).

Several hypotheses on the formation of the Ilímaussaq intrusion have been proposed. Sørensen (1970) considers three periods of consolidation: (1) augite syenite, (2) main body of agpaitic rocks and (3) lujavrites. The main body of agpaitic rocks developed from a gas-rich magma enclosed in the augite syenite. The following crystallization sequence has been recognized: pulaskite → heterogeneous foyaite → sodalite foyaite → naujaite. The kakortokites crystallized at the same time as these rocks within the bottom part of the agpaitic magma. The lujavrites either developed from a residual magma entrapped between the naujaites and the kakortokites or from a late magma injected in connection with subsidence of the earlier crystallized rocks. Engell (1973) favours a residual magmatic origin of the lujavrites. Larsen (1976) assumes the existence of several intrusive magmas: (1) an augite syenite magma, (2) a magma which produced the differentiation sequence: pulaskite → heterogeneous foyaite → sodalite foyaite → naujaite, (3) a magma from which the kakortokites crystallized and possibly (4) a magma from which the lujavrites developed.

A large number of *pegmatites* occur within the naujaites and the kakortokites of the Ilímaussaq intrusion. According to Sørensen (1962) pegmatites within the naujaites can be subdivided into simple and complex varieties. The former are either zoned or unzoned. They presumably crystallized from thin, conformable, low viscosity magma sheets or layers enclosed in partly or completely consolidated naujaite. The complex pegmatites contain late replacement bodies composed mainly of albite, analcime and/or natrolite. Generally small amounts of rare, exotic minerals are present. The bodies may represent the reaction product between mainly eudialyte-rich layers in the zoned pegmatites and percolating fluids expelled from lujavrite magmas. Ore minerals have not been found in the simple pegmatites, only in the complex varieties. They comprise galena, sphalerite and molybdenite. Westerveldite (FeAs) and loellingite have been found in specimens from two unclassified naujaite pegmatites.

Pegmatites within the kakortokites have not been studied in any detail. Unpublished observations by the author suggest a subdivision into: (1) huge microcline-rich (agpaitic) pegmatite dykes and sills with considerable amounts of aegirine and/or arfvedsonite, (2) large aegirine pegmatite dykes and (3) small microcli-

ne-aegirine-arfvedsonite pegmatite bodies often with natrolite-rich cores. Several of the first two mentioned varieties have been mapped by Bohse *et al.* (1971). Ore minerals have not been found within these two varieties. Small amounts of galena, sphalerite, loellingite and at one locality also native lead occur within the type 3 pegmatite variety. The mineralogy of one of these has been described briefly in Karup-Møller (1975).

A large number of *pneumatolytic-hydrothermal veins* occur mainly in naujaite. They are generally located near the contact between this rock type and lujavrites. The veins are dominated by one or several of the minerals: microcline, natrolite, analcime, albite, sodalite, ussingite, aegirine and arfvedsonite. A large number of rare minerals have been found in small amounts in many of these veins. These veins are considered to have crystallized from fluids expelled from crystallizing lujavrite.

MODE OF OCCURRENCE OF THE ILÍMAUSSAQ ORE MINERALS

Ore minerals in pegmatites and pneumatolytic-hydrothermal veins

The ore minerals identified in the Ilímaussaq pegmatites and pneumatolytic-hydrothermal veins have been described in several publications. Four major mineral associations have been recognized on the basis of their principal elements:

      I. Pb-Zn-Mo association
      II. Cu-Sb association
      III. Fe-As association
      IV. Fe-Ni-As-Sb association

All publications describing these four associations are listed in Table 1. The table includes: (1) the major minerals, (2) all primary and secondary hypogene ore minerals, and (3) all supergene ore minerals.

In Table 2 all hypogene and supergene ore minerals are classified according to their chemical composition and mode of formation. The ore mineralogy of the four associations is summarized below.

I. Pb-Zn-Mo association

Galena and sphalerite, not associated with other ore minerals, occur in trace amounts in nearly all complex pegmatites and pneumatolytic-hydrothermal veins. A mineralogical-geochemical study of the minerals from a large number of localities is currently in progress. Galena and sphalerite also occur with most of the ore minerals belonging to the three other associations.

Native lead associated with galena, sphalerite and loellingite has been found in a kakortokite pegmatite (locality 5, fig. 1) while native lead alone occurs as a thin

Table 1. Summary of literature describing ore minerals in the Ilímaussaq pegmatites and pneumatolytic-hydrothermal veins

	LOCALITIES	LITERATURE REFERENCE	LOCALITY DESCRIPTIONS	PRIMARY AND SECONDARY HYPOGENE ORE MINERALS	SUPERGENE ORE MINERALS
I	Pb–Zn–Mo ASSOCIATION				
1	Many localities.	Karup-Møller and Rose-Hansen (in prep.).	Pegmatites and hydro-thermal veins in nau-jaite, lujavrite, ka-kortokite and sodalite foyaite.	Sphalerite, galena and molybdenite.	Cerussite and hydroce-russite.
2	Kakortokites (Localities 5 and 6, fig. 1).	Karup-Møller (1975).	Pegmatite (not exposed) in kakortokite (loc. 5, fig. 1) and mineralized fault in the kakortokite border pegmatite (loc.6).	Three associations, crystallization se-quence indicated: sphalerite → native lead (1), galena → native lead (2) and loellingite → galena → native lead (3).	Litharge, plattnerite and hydrocerussite.
3	Kakortokite pegmatite. (Near loc. E, fig. 1).	Johnson (in prep.).	Natrolite-microcline peg-matite.	Helvite, sphalerite and galena.	
4	Kvanefjeld (Near loc. 1, fig. 1).	Metcalf-Johansen (1977).	Analcime veins in me-dium to coarse-grained lujavrite.	Willemite, sphalerite and galena.	
II	Cu–Sb ASSOCIATION				
	a. Cu–Sb subtype				
5	Taseq (loc. 1, fig. 1) (Type locality for cuprostibite and chalcothallite).	Semenov et al. (1967).	Ussingite veins in naujaite described by Engel et al. (1977).	Chalcothallite and vrbaite.	Avicennite(?).
6		Sørensen et al. (1969b).	–"–	Cuprostibite, loellingite, native silver, dyscrasite(?), argentite(?) and chal-copyrite(?).	Unidentified cuprostibite al-teration products.
7	–"–	Karup-Møller and Ma-kovicky (in prep.).	–"–	Chalcothallite – redescribed.	
8	Kangerdluarssuk pla-teau.	Karup-Møller et al. (1978).	Analcime-aegirine veins near lujavrite-naujaite contact.	Cuprostibite enclosing small amounts of dyscrasite, galena (decomposed) and loellingite.	
9	–"–	López Soler et al. (1976).	–"–	Cuprostibite (optical study).	
10	–"–	Karup-Møller (1978).	–"–	In silicate minerals surrounding the cu-prostibite aggregates: dyscrasite, allar-gentum, mineral A (a bindheimite va-riety ?), galena, sphalerite, cuprite and native copper.	Antimonian silver (variety silver-3), senarmontite, cuprite, native copper, chalcocite, digenite and cerussite(?).
11	Kvanefjeld (Locality 3, fig. 1. Type locality for rohaite).	Karup-Møller et al. (1978).	Analcime-aegirine vein along margins of trachyte dyke in me-dium to coarse grai-ned lujavrite.	Cuprostibite, allargentum, silver-1, sil-ver-2, (primary and exsolved from sil-ver-1), rohaite, chalcocite, (primary and secondary), high digenite (decom-posed), djurleite(?)(exsolved from dige-nite), sphalerite, galena (decomposed), cuprite and loellingite.	Antimonian silver (variety silver-3), senarmontite, chalcocite and digenite.
12	–"–	Karup-Møller (1978).	–"–	Rohaite, sphalerite, chalcocite and cuprite.	Digenite and senarmontite supergene after rohaite.
13	–"–	Karup-Møller (1978).	–"–	Chalcocite and high digenite. High digenite has decomposed to low digenite and chalcocite. Very rare exsolved djurleite(?) in dige-nite.	Covellite, blaubleibender covellite (2 varieties) and connellite after low digenite-chalcocite ag-gregates.
14	Kangerdluarssuk pla-teau and Kvane-fjeld (Locality 2, and 3, fig. 1).	Karup-Møller (1978).	See 8 and 11 above.		"Cuprite" (several varieties), "Sb-malachite", valentini-te, unidentified Sb-Cu mi-neral and native copper. (All after cuprostibite).
15	–"–	Karup-Møller (1978).	See 8 and 11 above.		
	b. Cu–Sb–S subtype				
16	Kangerdluarssuk pla-teau (Locality 2, fig. 1, 15 m from Cu-Sb mineraliza-tion). (Skinnerite type locality).	Karup-Møller (1974) and Karup-Møller and Makovicky (1974).	Analcime (–natrolite) veins in naujaite. Veins not exposed, only loose boulders in till.	Native antimony, senarmontite (partly replacing the native antimony), valen-tinite, skinnerite, Ag-tetrahedrite (=tetrahedrite-1), chalcostibite, galena (partly replaced by Cu-Sb-minerals), Ag-tetrahedrite decom-position mineral and traces loel-lingite.	
17	Tuperssuatsiait (Locality 4, fig. 1).	Karup-Møller (1974).	Natrolite-rich part of lujavrite vein in nau-jaite.	Ag-tetrahedrite (=tetrahedrite-1), Fe-Ag-tetrahedrite (=tetrahedrite-2), native antimony, senarmontite (partly repla-cing the native antimony), valentinite polybasite and traces famatinite. Sub-stantial amounts of early galena is partly replaced by argentite, covellite and Cu-Sb-ore minerals. Sphalerite only by Cu-Sb-ore minerals.	
III	Fe–As ASSOCIATION				
18	Many localities (A–G, fig. 1).	Karup-Møller and Makovicky (1977).	Pegmatites and hydrothermal mineral veins in naujaite, lujavrite, kakortokite and sodalite foyaite.	Westerveldite (loc. A-D, fig. 1), wester-veldite alteration products (loc. A), loellingite (A-E), galena (A-G) and na-tive antimony (B). Crystallization se-quence at loc. A-C : westerveldite → loellingite. At loc. D : loellingite → westerveldite.	Beudantite (Loc. E, fig. 1).
IV	Fe–Ni–As–Sb ASSOCIATION				
19	Igdlúnguaq pen-ninsula (Loca-lity 7, fig. 1).	Oen and Sørensen (1964). Oen et al. (1977).	Disseminations in naujaite adjacent to intrusive lujavrite.	Primary : galena, skutterudite, niccolite and breithauptite. Secondary hypogene : gudmundite and Ni-westerveldite (for-mer maucherite?).	

Table 2. Ore minerals in pegmatites and pneumatolytic-hydrothermal veins

A. HYPOGENE ORE MINERALS

I Pb–Zn–Mo association.....................	Sphalerite, galena, native lead and molybdenite.

II Cu–Sb association

Group 1. Cu–Sb–Ag alloy minerals.........	Cuprostibite, dyscrasite, allargentum, antimonian silver (2 varieties : silver–1 and silver–2), and native copper.
2. Cu–sulphides	Chalcocite (2 generations), digenite, djurleite(?) and covellite.
3. Cu–Sb–Ag–Fe sulphides............	Skinnerite, chalcostibite, Ag–tetrahedrite (tetrahedrite–1), Ag–Fe–tetrahedrite (tetrahedrite–2), unknown Ag–tetrahedrite decomposition mineral, famatinite, polybasite and argentite.
4. Tl–sulphides......................	Chalcothallite, rohaite and vrbaite(?).
5. Cu–Fe–(Sn) sulphides.............	Chalcopyrite, pyrite and stannite(?).
6. Cu–Sb oxides....................	Valentinite, senarmontite, cuprite and mineral A (a bindheimite variety?).

III Fe–As association	Loellingite, westerveldite and westerveldite alteration products.
IV Fe–Ni–As–Sb association.....................	Skutterudite, niccolite, breithauptite, gudmundite, Ni–westerveldite and Ni–loellingite.

B. SUPERGENE ORE MINERALS

I Oxides......................................	Senarmontite, unidentified Sb–Cu hydroxide(?) associated with senarmontite, cuprite, litharge, plattnerite and avicennite(?).
II Carbonates, sulphates and silicates............	Sb–malachite, cerussite, hydrocerussite, connellite brochantite, linarite, beudantite, crysocolla(?) and azurite(?).
III Native elements............................	Antimonian silver (variety silver–3) and native copper.
IV Cu–sulphides................................	Digenite, covellite, chalcocite and blaubleibender covellite (2 varieties).

crust on the surface of a fault cutting the kakortokite border pegmatite (locality 6). A detailed description is given by Karup-Møller (1975).

Molybdenite is an accessory ore mineral in the complex pegmatites. It very rarely occurs in the pneumatolytic-hydrothermal veins, e.g. at locality E in fig. 1 (Karup-Møller & Makovicky, 1977).

— — II. Cu-Sb association

The major elements of association II are Cu and Sb associated with minor Pb, Zn, Ag, Tl and traces of As. The association has been subdivided into the Cu-Sb subtype IIA and the Cu-Sb-S subtype IIB. The ore minerals belonging to subtype IIA have been found at the localities 1, 2a and 3 (fig. 1), while those belonging to the subtype IIB occur at the localities 2b and 4. Localities 2a and 2b lie at a distance of approximately 15 m from each other (fig. 13 in Karup-Møller, 1974). At each locality all ore minerals do not neccessarily occur in mutual association.

Cuprostibite is the major subtype IIA ore mineral. The following mineral parageneses have been recognized at the three cuprostibite localities: (a) cuprostibite enclosing rohaite ($TlCu_5SbS_2$), antimonian silver (variety silver (1)), dyscrasite, chalcocite, galena and/or loellingite, (b) silver (1) enclosing rohaite, primary cup-
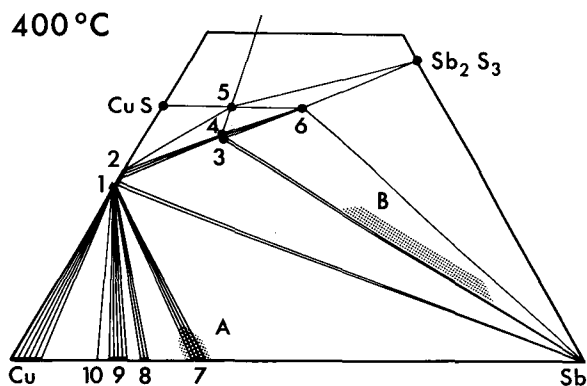
400 °C

Fig. 2. Cu-Sb-S phase diagram at 400°C modified after Skinner *et al.* (1972). 1: chalcocite, 2: digenite, 3: skinnerite, 4: tetrahedrite, 5: famatinite, 6: chalcostibite, 7: cuprostibite, 8-10: synthetic phases with no natural equivalents. The dotted areas represent the estimated range in bulk chemical composition of the Cu-Sb subtype IIA (A) and the Cu-Sb-S subtype IIB (B).

rite, chalcocite, cuprostibite and/or loellingite, (c) dyscrasite-allargentum intergrowth as host for galena, sphalerite, native copper and mineral A (possibly a bindheimite variety), (d) rohaite, chalcocite and/or sphalerite, (e) digenite and/or sphalerite and (f) complex intergrowths of silver (1), silver (2) and allargentum.

In the two sulphide-oxide occurrences (subtype IIB), the characteristic parageneses at locality 2b are (a) native antimony, skinnerite, chalcostibite, Ag-tetrahedrite (tetrahedrite-1), Sb-oxides (senarmontite, valentinite), galena and sphalerite and (b) skinnerite, chalcostibite, Ag-tetrahedrite and valentinite. Paragenesis (b) crystallized along shrinkage fractures in (a) and is therefore considered to have formed later. At locality 4 the paragenesis is native antimony, Fe-Ag-tetrahedrite (tetrahedrite-2), Ag-tetrahedrite, famatinite, polybasite, Sb-oxides (valentinite, senarmontite), galena and sphalerite. Famatinite is present only in extremely small amounts. At both localities the native antimony has been partly replaced by hypogene senarmontite.

Close agreement between some of the natural parageneses and experimental results within the systems Cu–Sb–S and Ag–Sb has been recognized.

The system Cu–Sb–S. The Ilímaussaq Cu-Sb mineral occurrences most probably crystallized at temperatures between 450°C and 350°C. The Cu-Sb-S phase system at 400°C shown in fig. 2 has been reproduced (with slight modifications) from Skinner *et al.* (1972). The most characteristic feature of the Ilímaussaq Cu-Sb association is the presence of the two new minerals skinnerite (Cu_3SbS_3) and cuprostibite (Cu_2Sb). Both are known from synthetic studies.

The synthetic analogue of skinnerite (phase 3 in fig. 2) is orthorhombic. It was experimentally produced by Skinner *et al.* (1972). At temperatures below 359°C skinnerite is not stable and decomposes into tetrahedrite, chalcostibite and antimony. The orthorhombic form of skinnerite is not quenchable due to a too rapid metastable polymorphic transformation into a monoclinic form at 122°C. The quenched product at room temperatures is always the monoclinic form.

The content of silver and iron in the two Cu-Sb-S parageneses excludes compar-
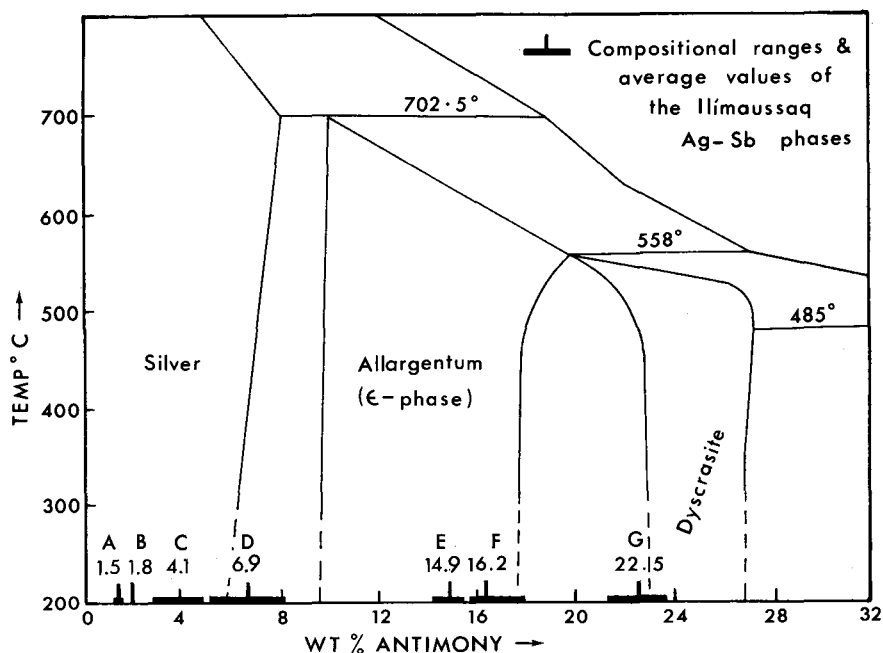
Fig. 3. Ag-Sb phase diagram modified after Somanchi (1966) with compositional ranges and average values of the Ilímaussaq Ag-Sb phases. G, F and B: dyscrasite, allargentum and supergene antimonian silver(3) at locality 2a in fig. 1. E: allargentum. C: silver(1), D: silver(2) and A: supergene antimonian silver(3) at locality 3 in fig. 1.

ison between mineral parageneses and phase associations in the pure Cu–Sb–S system.

Synthetic cuprostibite is stable at temperatures below 586°C. The association of cuprostibite with chalcocite in the Ilímaussaq Cu-Sb mineral occurrences is thus in agreement with the experimental results in fig. 2. The phase diagram also explains the apparent non-existence in the Ilímaussaq intrusion of cuprostibite with Cu-Sb sulphides.

Cuprostibite has not (yet) been observed in association with either native antimony or natural equivalents to the synthetic phases plotting between Cu_2Sb and Cu in fig. 2.

The estimated compositional ranges of the fluids leading to the formation of the Ilímaussaq Cu-Sb-(S) ore mineral associations are indicated by the dotted areas in fig. 2.

The system Ag–Sb. Synthetic studies in this system were carried out by Somanchi (1966), and natural occurrences from Cobalt, Ontario were described by Petruk *et al.* (1970, 1971) and others. The chemical compositions (average values and ranges) of all the Ilímaussaq Ag-Sb-varieties (localities 2a and 3, fig. 1) are plotted in fig. 3.

At locality 2 a (fig. 1) dyscrasite ($Sb_{0.20}Ag_{0.80}$) (G, fig. 3) intergrown with allargentum ($Sb_{0.15}Ag_{0.85}$) (F, fig. 3) may have crystallized penecontemporaneously (Karup-Møller, 1978). At locality 3 (fig. 1) silver (2) ($Sb_{0.06}Ag_{0.94}$) (D, fig. 3) contains exsolved lamellae of allargentum ($Sb_{0.14}Ag_{0.86}$) (E, fig. 3) and of silver (1) ($Sb_{0.04}Ag_{0.96}$) (C, fig. 3). Silver (1) also crystallized as a primary mineral in contact with silver (2) before the decomposition of the latter took place (Karup-Møller, 1978). At both Ilímaussaq localities supergene alteration of the hypogene Ag-Sb minerals has resulted in the formation of Sb-poor antimonian silver (silver-3). The composition of silver (3) from locality 2a is given as B in fig. 3 and from locality 3 as A in fig. 3.

The mineral relationships observed closely resemble those described by Petruk *et al.* (1970, 1971) on natural materials from Cobalt. These, however, contain small amounts of mercury. The apparent penecontemporaneous crystallization of the two antimonian varieties at locality 3 in fig. 1 (analyses C and D in fig. 3) is at variance with the experimental results by Somanchi (1966) which are also shown in fig. 3. The natural assemblages (both from Cobalt and Ilímaussaq) also suggest a much narrower compositional field of allargentum than that suggested by the experimental data in fig. 3.

III. Fe-As association

This association comprises westerveldite and loellingite (Karup-Møller & Makovicky, 1977). The two minerals occur both in pegmatites and pneumatolytic-hydrothermal veins. At some localities westerveldite is partly replaced by loellingite (A-C, fig. 1), while this relationship is reversed at locality D. At localities E-G the only arsenide present is loellingite. Galena occurs at most of the localities, sphalerite and molybdenite at a few localities but native antimony only at locality B.

At locality A alteration of westerveldite has resulted in the formation of an extremely fine-grained secondary westerveldite intergrown with an unidentified hexagonal phase. This material has been termed the 'westerveldite alteration product'.

IV. Fe-Ni-As-Sb association

This association has only been found in extremely small amounts at locality E, fig. 1 (Oen & Sørensen, 1964; Oen *et al.* 1977). The ore minerals occur in naujaite within a restricted area a few square centimetres in size. They lie along fractures in sodalite and aegirine at a short distance from an acmite-arfvedsonite vein cutting the naujaite. An early generation of galena, skutterudite, niccolite and breithauptite has subsequently been replaced by loellingite, gudmundite and Ni-westerveldite (originally described as maucherite).

Supergene ore minerals

Supergene alteration of cuprostibite has resulted in the formation of nearly pure cuprite, several hydrated 'cuprite' varieties with variable contents of Sb, Pb, Si and senarmontite together with an unidentified mineral, Sb-malachite and native copper (Karup-Møller, 1978). At locality 2a supergene alteration of dyscrasite and allargentum in association with cuprostibite has resulted in the formation of antimonian silver, senarmontite, cuprite and native copper (Karup-Møller *et al.*, 1978). At locality 3, the alteration of allargentum, silver (1) and silver (2) has resulted in development of silver (3) (fig. 3) and senarmontite (Karup-Møller, 1978). At locality 2a digenite and chalcocite have replaced galena while at locality 3 the only mineral replacing galena is chalcocite.

Alteration of low digenite intergrown with chalcocite at locality 3 has resulted in the formation of connellite, covellite and two varieties of blaubleibender covellite (Karup-Møller, 1978). At locality 2a cavities less than one centimetre in size are filled with secondary senarmontite, connellite, brochantite and linarite (Karup-Møller, 1978). Sørensen *et al.* (1969b) have described chrysocolla as a cuprostibite decomposition product at locality 1. At the same locality chalcocite and (?) avicennite are secondary after chalcothallite (Semenov *et al.* 1967). At locality 6 plattnerite represents a supergene decomposition product after native lead and at locality 5 hydrocerussite and litharge are supergene after the native lead (Karup-Møller, 1975). According to Semenov *et al.* (1967) cerussite is secondary after galena. Beudantite has resulted from the decomposition of intergrown loellingite and galena at locality E (Karup-Møller & Makovicky, 1977). Alteration of rohaite to digenite and senarmontite may either be hypogene or supergene (Karup-Møller, 1978).

Accessory rock forming ore minerals

The ore minerals in heavy mineral concentrates from seven rock types have been studied (fig. 4). Sample locations are shown on fig. 1.

Each rock sample weighed about 35 kg and was obtained from the least weathered rock by careful outcrop search followed by blasting. About 7 to 12 kg of each were crushed and the heavy minerals were extracted from the fraction between 80 and 240 mesh.

All ore minerals identified are listed in fig. 4. The sample number e.g. '154327-5' stands for 'polished section of heavy mineral concentrate fraction no. 5 isolated from sample GGU 154327'. The only exception is 150130A-E which consists of chip samples of the naujaite sample GGU 150130. The term 'lujavrite MC' describes 'medium to coarse-grained lujavrite'.

The microprobe analyses (Tables 3-6 and 10) were completed with a Hitachi model XMA-5B microprobe at the Institute of Mineralogy, University of Copenhagen. Standards were synthetic troilite (for both Fe and S), natural PbS (for Pb only), natural NaCl (for Cl only), natural adularia (for K only), and pure synthetic As, Sb, Ni, Co, Sn and Cu. Corrections have been made according to a modified programme after Springer (1967).

The estimated standard deviation used in tables 3 to 6 describes the spread of analyses completed on a suite of mineral grains with standard measurements taken before and after each sequence.

Fig. 4.

Legend:
- · 1 - 5 grains counted
- • 6 -15 grains counted
- ⬤ 16-25 grains counted
- ● >25 grains counted

Mineral	Augite syenite (154332)	Alkali granite (154379)	Sodalite foyaite (154352)	Naujaite (57041)	Black kakortokite (154338)	Red kakortokite (154326)	White kakortokite (154327)	Green lujavrite (154359)	Lujavrite MC (154724)
Sphalerite		●	●	●	·	•	●	●	●
Galena		●	●	●	·		●	●	●
Troilite / pyrrhotite	●		•	•		·	·		
Djerfisherite			·	●			·		
Pyrite	·		·		·	·	·	·	
Marcasite						·			
Molybdenite			•	●			·		●
Chalcopyrite	●				·		·		
Loellingite		●	•		·	⬤		·	
Westerveldite		•	•		·	●			
Seinäjokite									●
Gudmundite									●
Native Sn					·	•	·		
Native Pb					•	•	·		●
Native Fe						·	●		●
Unknown Pb-Sn-(Cu) min.							·		
Magnetite	•	⬤	·		•	⬤			●
Hematite	•	●	•			⬤			·
Ilmenite	⬤	•		·					
Chromite					·				
Ulvöspinel	⬤								
Rutile	·						●		
Decomposed wüstite							·	●	

Fig. 4. Content of accessory hypogene ore minerals in some of the major rock types of the Ilímaussaq intrusion. Decomposed wüstite, native iron and associated magnetite, native tin and associated unknown Sn-Cu(-Pb) phase may represent contaminated material.

Sphalerite

Sphalerite is a common accessory mineral found in nearly all the Ilímaussaq rocks (fig. 4). The content of iron in sphalerite from different rocks determined by the microprobe is listed in Table 3.

Sufficient amounts of sphalerite were present in heavy mineral concentrates from the

Table 3. Microprobe analyses for Fe in sphalerite

Polished section No.	Host rock	No. grains analyzed	Wt. % Fe range	Wt. % Fe av.	esd
154352-25	Sodalite foyaite	10	1.0- 2.5	1.9	0.4
57041-2	Naujaite	14	9.6-14.1	11.8	1.4
154326-12	Red kakortokite	6	1.8- 2.0	1.8	0.1
154327-8	White kakortokite	9	11.3-14.5	13.2	0.9
154359-1	Green lujavrite	11	2.4- 4.4	3.1	0.5
154724-14	Lujavrite MC	11	0.3- 2.2	1.1	0.5

esd estimated standard deviation

green lujavrite and the lujavrite MC for emission spectral analyses. The following results were obtained (ppm):

154359-1   (green lujavrite) Cd 20, Mn 1000, In 8

154724-14 (lujavrite MC)   Cd 50, Mn 700, In 10

In the green lujavrite, sphalerite grains often lie in contact with galena which has sometimes been partly altered into hydrocerussite (fig. 5). Sometimes the sphalerite is enclosed in the galena.

In the white kakortokite (154327-4) one sphalerite grain contained very fine-grained, exsolved chalcopyrite. In the same polished section, sphalerite sometimes lies in contact with aggregates of pyrite and magnetite (presumably decomposed troilite as described below and illustrated in fig. 10).

Sphalerite in the alkali granite contains small inclusions of ilmenite, hematite and rutile.

Sphalerite in the naujaitite is often cut by limonite-filled fractures. It has been found in mutual contact with troilite and appears to have crystallized in equilibrium with this mineral.

Galena and associated native lead

After sphalerite, galena is the most common of the accessory ore minerals. Supergene alteration of galena has resulted in the formation of hydrocerussite. The replacement has generally taken place along the galena cleavage directions. Remnants of galena may lie embedded in the secondary mineral (fig. 5). Isolated grains of hydrocerussite with no inclusions of galena or other minerals were identified by X-ray diffraction: In the green lujavrite sphalerite is sometimes enclosed in galena. Galena may contain inclusions of westerveldite and loellingite (white kakortokite and lujavrite MC). in the lujavrite MC galena is commonly associated with native lead. The native lead is either enclosed in the galena or interstitial to this mineral (fig. 6). Often the native lead is replaced by litharge without galena being affected. On the other hand, the replacement of galena by hydrocerussite (fig. 7) may not essentially have affected the native lead. However, litharge after native lead is always in part replaced by hydrocerussite when the adjacent galena is replaced by this mineral (fig. 8). At the same time or later secondary galena may have formed, marking the
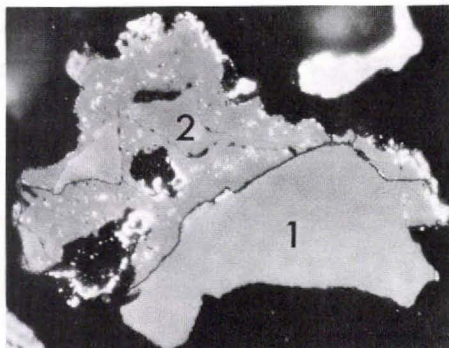
Fig. 5. Sphalerite (1) in contact with hydrocerussite (2) supergene after galena. White specks are galena remnants (GGU 154359-1. × 100. Oil immersion).

boundary between the two original minerals (figs 7 and 8). Alteration of the two primary minerals is considered to be supergene, although this cannot be proved.

The relationships between galena, native lead and their respective alteration products in the lujavrite MC closely resemble the relationships between the same minerals in the PbS-Pb association found in the kakortokite pegmatite described by Karup-Møller (1975).

Troilite and type 5.63C-pyrrhotite

Pure troilite occurs in the naujaite, the white kakortokite and the sodalite foyaite. Troilite (pyrrhotite 2C) with exsolved type 5.63C-pyrrhotite is a common accessory sulphide in the augite syenite (fig. 4).

Naujaites. Troilite is frequently seen as 'rusty' spots on weathered naujaite surfaces. In chip samples (150130 A-E) the sulphide is enclosed in microcline, arfvedsonite and altered eudialyte. Intense supergene alteration of the troilite has resulted in an extremely fine-grained mixture of marcasite and limonite in variable proportions. Bird's-eye textures are often developed, sometimes concentrically around a few relatively large and platy marcasite crystals (fig. 14).

In 57041-2 troilite occurs in contact with djerfisherite and sphalerite. Marcasitization of the troilite is rare, but grains are frequently cut by limonite-filled fractures.
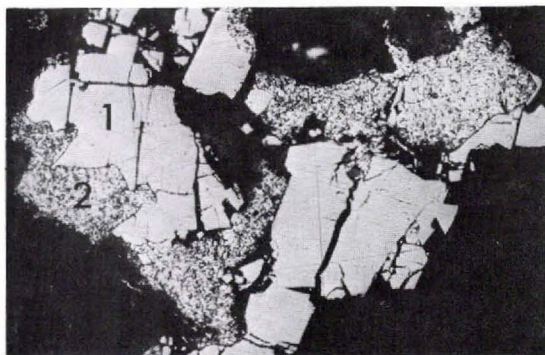

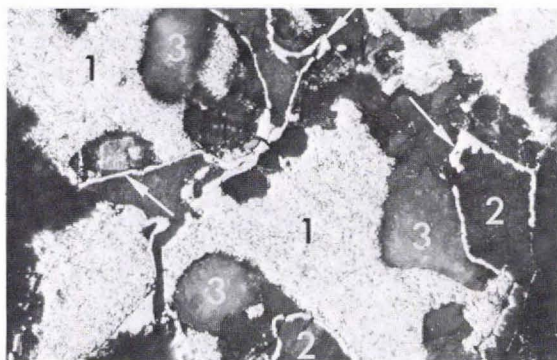Fig. 6. Galena (1) corroded by native lead (2). (GGU 154724-29. × 560).

Fig. 7. Native lead (1) originally crystallized in contact with galena which has now been completely altered to hydrocerussite (2). Slight replacement of the native lead by litharge (3) has taken place. Secondary galena (at arrows) marks the original galena-native lead boundary. (GGU 154724-29. × 930. Oil immersion).

Microprobe analyses on troilite in 57041-2 and in 150130-E are listed in Table 4. The former are plotted in fig 9E. Single crystal studies (Weissenberg and precession) on a troilite fragment removed from 57041-2 have confirmed the identity of the mineral.

White kakortokite and sodalite foyaite. A few of the troilite grains in the white kakortokite are intergrown with djerfisherite but most of them are not found in contact with other ore minerals (154327-4). Aggregates of pyrite and magnetite, sometimes together with sparse chalcopyrite, may represent the hypogene oxidation product of an original pyrrhotite (6 FeS + $2O_2 \rightarrow 3FeS_2 + Fe_3O_4$). The magnetite is equigranular to rectangular in shape and is uniformly embedded in pyrite. One of the aggregates (fig. 10) is penetrated by late troilite (analyzed by microprobe) and galena. In one aggregate sparse chalcopyrite was observed.

A few troilite grains were identified in 154352-18 from the sodalite foyaite. One grain was found in contact with djerfisherite.

Microprobe analyses on troilite in the white kakortokite and in sodalite foyaite are listed in table 4 and plotted in figs 9 F and 9 D respectively.

Augite syenite. In the medium to strongly magnetic heavy mineral concentrates from the augite syenite, troilite occurs as the host for exsolved pyrrhotite (type 5.63C). The intergrowth is assumed to represent the decomposition product of a high temperature hexagonal (1C) pyrrhotite variety. The troilite host (and therefore also the original pyrrhotite 1C) ranges in shape from rectangular to perfectly oval grains. A few of these have been found enclosed in olivine. It is therefore concluded that the sulphides crystallized from immiscible
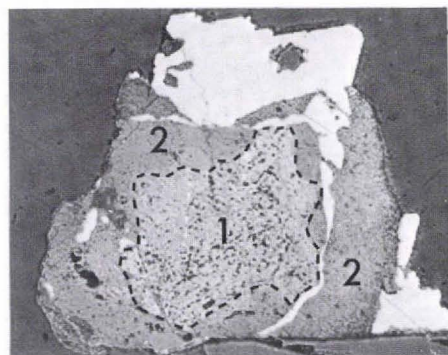

Fig. 8. Native lead originally crystallized in contact with galena. The native lead was first replaced by litharge (1). Late hydrocerussite (2) has replaced both galena and litharge. A string of secondary galena marks the original native lead - galena boundary. (GGU 154724-29.× 125. Air).

Table 4. Microprobe analyses on troilite and type 5.63C-pyrrhotite

Rock type		GGU No.	Number of analyses	Fe wt. %	esd	S wt. %	esd	Total	Molar ratio Fe : S
Augite syenite									
aggregate no.	1	154332-15	3	62.16	0.88	38.66	0.58	100.82	48.00 : 52.00
	2	154332-15	3	62.17	0.09	38.72	0.12	100.89	47.00 : 52.03
(exsolved	3	154332-15	3	62.24	0.32	38.94	0.20	101.18	47.85 : 52.15
type 5.63	4	154332-15	3	61.29	0.52	38.64	0.14	99.93	47.66 : 52.34
pyrrhotite)	5	154332-16	3	61.14	0.23	38.86	0.07	100.00	47.46 : 52.54
	6	154332-16	3	61.79	0.04	38.92	0.04	100.71	47.69 : 52.31
average	1-6		18	61.80	0.48	38.79	0.13	100.59	47.77 : 52.23
aggregate no.	1	154332-15	3	64.45	0.32	37.04	0.32	101.49	49.98 : 50.02
	2	154332-15	3	64.04	0.09	36.48	0.08	100.52	50.19 : 49.81
	3	154332-15	3	64.33	0.38	36.90	0.30	101.23	50.02 : 49.98
(host troi-	4	154332-15	3	63.52	0.02	36.50	0.08	100.02	49.98 : 50.02
lite)	5	154332-16	3	62.94	0.55	36.25	0.23	99.19	49.92 : 50.08
	6	154332-16	4	63.03	0.66	36.64	0.28	99.67	49.69 : 50.31
average	1-6		19	63.72	0.65	36.64	0.29	100.35	49.96 : 50.04
Augite syenite		154332-18	10	63.47	0.81	36.91	0.71	100.38	49.68 : 50.32
Sodalite foyaite		154332-5	10	64.05	0.44	36.82	0.25	100.87	49.97 : 50.03
Naujaite		57041-2	20	64.54	0.61	36.86	0.33	101.40	50.13 : 49.87
Naujaite		150130-E	2	64.50	0.23	37.02	0.41	101.52	50.01 : 49.99
White kakortokite		154327-4	15	63.72	0.48	36.74	0.38	100.46	49.89 : 50.11

esd estimated standard deviation.

sulphide droplets in the augite syenite magma. The exsolved pyrrhotite is irregularly patchy in shape when the host is cut perpendicular to the X-ray crystallographic *c* axis of the mineral, and irregularly lamellar in shape when cut parallel to the *c* axis. The visually estimated proportion between the host and enclosed variety is 3:1.

In the least magnetic sulphide fraction (154332-18) most of the troilite grains are mono-mineralic.

Microprobe analyses were completed on six host troilite aggregates and enclosed exsolved pyrrhotite in 154332-15 and 154332-16. Each phase was analysed at three different points (Table 4, figs 9 A and 9 B). Ten monomineralic troilite grains in 154332-18 were also analyzed (Table 4, fig. 9 C). A few of the least iron-rich analyses plotted in fig. 9 C may in part represent undetected exsolved pyrrhotite.

An emission spectrographic analysis on troilite-pyrrhotite from the augite syenite gave 200 ppm Co and less than 5 ppm Ni. The presence of these two elements in troilite from the agpaitic rocks could not be detected by microprobe.

Single crystal studies on a troilite grain with exsolved pyrrhotite extracted from 154332-15 gave two perfectly parallel oriented lattices. One, a troilite lattice, is identical with that obtained on the troilite fragment removed from 57041-2.
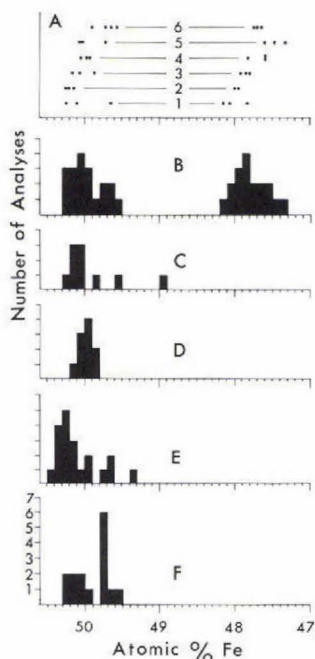
Fig. 9. A: Plot of individual analyses on troilite and exsolved type 5.63C pyrrhotite in six aggregates (1-6) in augite syenite (GGU 154374-31 and -33). B-F: Frequency histograms showing composition versus number of analyses. B: Composite histogram of all analyses plotted in A. C: Augite syenite (GGU 154374-18). D: Sodalite foyaite (GGU 154352-18). E: Naujaite (GGU 57041-2). F: White kakortokite (GGU 154327-8).

Morimoto *et al.* (1975) have described some pyrrhotites of nonintegral type, the nC-pyrrhotites. The chemical compositions of these lie between that of Fe_9S_{10} (atomic % Fe 47.20) and $Fe_{11}S_{12}$ (Fe 47.80 %). Careful study of the 0-level (A*-C* plane) Weissenberg photographs recorded on the augite syenite troilite and on exsolved pyrrhotite have shown that the lattice of the latter represents a nonintegral pyrrhotite with $n = 5.63 \pm 0.02$ Å. Intergrowth of natural troilite (pyrrhotite 2C) with pyrrhotites 5.72C to 5.75C is described by Morimoto *et al.* (1975).

Exact cell dimensions could not be obtained on the Ilímaussaq pyrrhotite. The number of diffraction lines in the Guinier photographs are not sufficient for refinement of the cell dimensions. The single crystal study has revealed the complete equivalence of the A-cell
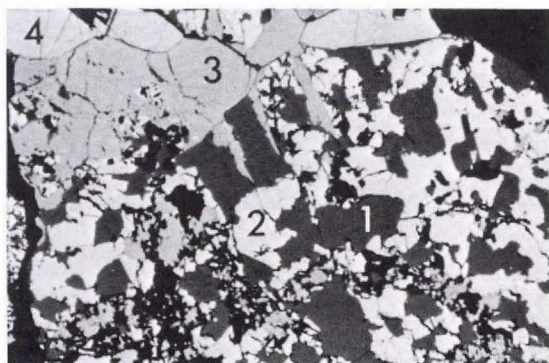

Fig. 10. Aggregate (decomposed troilite?) of magnetite (1) in pyrite matrix (2) is injected by late troilite (3) and galena (4). (GGU 154327-4. × 285. Oil immersion).

dimension for troilite and exsolved 5.63C-pyrrhotite. However, the C dimensions are different. Assuming that the cell dimensions for the Ilímaussaq troilite are identical with those published for the mineral (e.g. Craig & Scott, 1974: A 3.444 Å, C 5.875 Å) then $\triangle$C for troilite and exsolved 5.63C-pyrrhotite is 0.134 Å. This yields a cell dimension of C 5.742 Å for the exsolved variety. According to Morimoto et al. (1975, fig. 10) this value corresponds to a pyrrhotite with n = 5.21, which is considerably below the value 5.63 measured on the Weissenberg films. According to fig. 10 in their paper a value of n = 5.63 corresponds to a pyrrhotite with 47.72 % Fe. The microprobe analyses on the augite syenite pyrrhotite gave 47.77 % (Table 4). The Fe content corresponding to n = 5.21 is 47.52 % according to their fig. 10.

Djerfisherite

This mineral is known in the literature only from three terrestrial localities. It was originally observed in meteorites by Ramdohr (1963, mineral C) but first described in detail by Fuchs (1966), who found it embedded in enstatite-bearing chondrites. Later djerfisherite was found at two localities in the USSR.

Genkin et al. (1969) have described djerfisherite associated with Cu-Ni sulphides at the Talnakh deposit, Norilsk. The mineral is associated mainly with cubanite, talnakite and pyrrhotite. According to Sokolova et al. (1971) djerfisherite isolated in silicate minerals or intergrown with pyrrhotite, cubanite, pentlandite and other sulphides, is a relatively common mineral in the potassium feldspar-nepheline-aegirine pegmatites of the Khibina massifs of the Kola Peninsula. Semenov (1972) has not reported finding djerfisherite in the Lovozero intrusion.

Djerfisherite is a common accessory ore mineral in the naujaites of the Ilímaussaq intrusion, (fig. 4). It has also been found intergrown with pyrrhotite in the kakortokites (154327-4) and in sodalite foyaite (154352-2 and 154352-18).

Djerfisherite is isotropic. In reflected light it has a dull olive-khaki colour. The polishing hardness is distinctly lower than that of the associated troilite.

Microprobe analyses were carried out on 11 mineral grains in 57041-2 (Table 5). The contents of Cl, K and S recorded on each grain, vary within narrow limits. The contents of Fe and Cu vary in such a way that limited substitution between the two elements has obviously taken place. Na was present in amounts less than 0.2 per cent.

The following composition for djerfisherite was published by Fuchs (1966): Fe 50.7, S 33.8, K 8.7, Cu 4.2, Cl 1.0, Ni 0.8, and Na 0.3 wt. per cent, summing at 99.5. According to Fuchs some members of the Commission for New Minerals and Mineral Names considered the Cl to have no place in the structure of a sulphide mineral. Fuchs therefore assumed that the presence of Cl was caused by unobserved inclusions of lawrencite ($FeCl_2$).

Djerfisherite from the two Soviet localities has apparently not been analyzed for Cl. Similar values for K and S were obtained on all analyzed djerfisherite (this study and others). The content of Cu in some of the Soviet varieties reached 15 per cent and the content of Fe was correspondingly lower. These analyses thus support the limited substitution between Cu and Fe suggested above.

The ideal formula for djerfisherite proposed by Fuchs (1966) is: $K_3(Na, Cu) (Fe, Ni)_{12}S_{13}$ (Z =3, $d_{cal.}$ = 3.9 gm/cm^3). The formula for djerfisherite from the Ilímaussaq intrusion

Table 5. Microprobe analyses on djerfisherite

Grain No.	K Wt. %	Fe Wt. %	Cu Wt. %	Cl Wt. %	S Wt. %	Sum
1	8.8	46.8	8.3	1.3	33.5	99.7
2	8.3	48.5	6.1	1.4	33.6	97.9
3	8.2	48.6	7.8	1.5	33.8	99.9
4	8.2	48.8	8.6	1.4	33.3	100.3
5	8.3	48.9	6.5	1.4	33.8	98.9
6	8.8	49.0	7.2	1.4	34.0	100.4
7	8.4	49.0	5.8	1.3	34.1	98.6
8	8.3	50.0	5.3	1.4	33.9	98.9
9	8.5	50.4	5.7	1.4	33.0	99.0
10	8.3	50.7	5.5	1.3	33.2	99.0
11	8.7	51.8	3.8	1.4	34.4	100.1
Average	8.4	49.3	6.4	1.4	33.7	99.2
esd	0.2	1.3	1.4	0.1	0.4	

esd estimated standard deviation.
GGU sample no. 57041-2.

based on a content of S equal to 13 is: $(K_{2.66}Fe_{10.92}Cu_{1.25}Cl_{0.49})\ S_{13.0}$ ignoring the small contents of Na (<0.2 per cent) present.

The cell dimensions of djerfisherite (Fuchs, 1966) are close to those of pentlandite (a 10.03 Å). Accordingly, Strunz (1970) has classified the mineral as a pentlandite variety. Using the pentlandite formula $[(Fe, Ni)_9S_8]$ the djerfisherite analyses in Table 5 can be written as: $(K_{1.64}Fe_{6.72}Cu_{0.77}Cl_{0.30})S_{8.00}$ with $d_{cal.} = 4.97$ g/cm^3 and Z = 4.

In 150130 A-E (described above) small grains of djerfisherite (less than 0.2 mm in size) have crystallized in contact with the troilite, enclosed in this mineral or isolated in adjacent silicate minerals. Supergene alteration of troilite and associated djerfisherite has taken place.
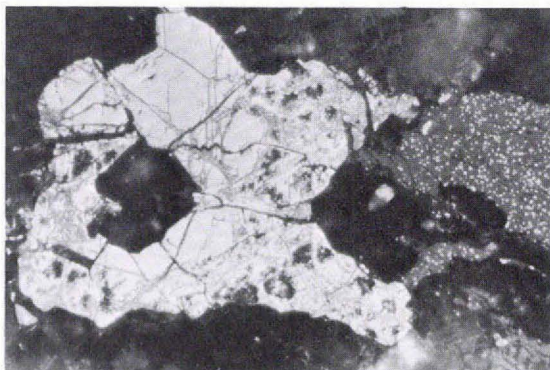

Fig. 11. Partial supergene alteration of djerfisherite, enclosed in microcline, has resulted in a very fine-grained mixture of granular pyrite (bright white), lamellar magnetite (grey) and unidentified dark reflecting substance (GGU 154130-B. × 525. Oil immersion).

Fig. 12. Partial supergene alteration of djerfisherite (white), enclosed in microcline, has resulted in a lamellar network of limonite. (GGU 154130-B. × 635. Oil immersion).

In fig. 11 djerfisherite, isolated in microcline, has been replaced by very fine-grained lamellar magnetite and granular pyrite associated with small amounts of an unidentified, dark reflecting substance (DRS below). The djerfisherite shown in fig. 12 has been almost completely replaced by limonite.

Fig. 13 covers most of an original djerfisherite grain in contact with unaltered troilite (1). Decomposition of the djerfisherite grains has taken place stepwise. (a) Lamellae of magnetite (dark grey, 4) and hematite (grey, 3) developed parallel to presumably (111). (b) Areas of djerfisherite between the lamellae were then almost completely altered to a very fine-grained mixture of pyrite and DRS (5). Remnants of djerfisherite (2) are enclosed in this material. (c) The fine-grained pyrite and associated DRS may then have been replaced by dense limonite (6). This limonite formation advanced from the contact of the original djerfisherite-microcline boundary (to the right of the photographed area). Nearly all lamellae in the limonite are themselves composed of limonite. If originally composed of magnetite and hematite the lamellae must later have been altered to limonite. The magnetite lamellae enclosed in the dense limonite near the area of fine-grained pyrite have thus escaped

Fig. 13. Almost complete supergene alteration of djerfisherite (2) in contact with pyrrhotite (1) has resulted in the formation of very fine-grained pyrite associated with unidentified dark reflecting substance (5), limonite (6), recrystallized pyrite (8) and lamellae of hematite (3), magnetite (4) and limonite (7). For detailed description see the text. (GGU 150130-D. × 505. Oil immersion).
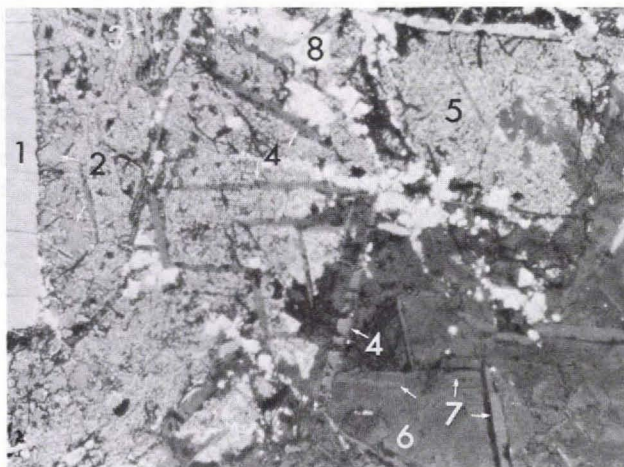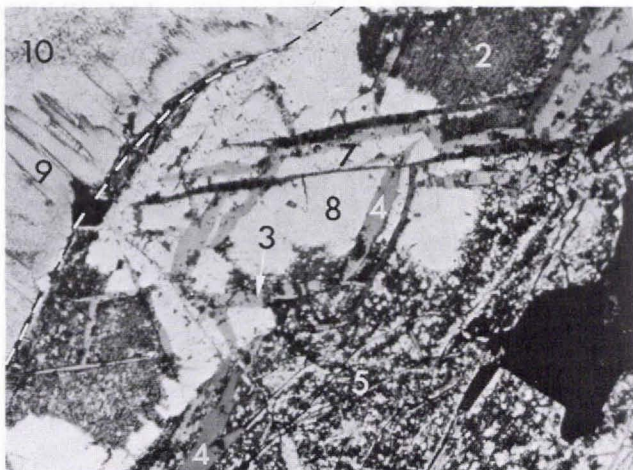
Fig. 14. Stippled line marks the boundary between original pyrrhotite and djerfisherite. The pyrrhotite has been altered (supergeneously) to platy marcasite (9) concentrically surrounded by a mixture of extremely fine-grained marcasite and limonite (10). Possibly at the same time, djerfisherite (2) has been replaced by a mixture of very fine-grained pyrite and an unidentified dark reflecting substance (5) cut by lamellae of hematite (3), magnetite (4) and limonite (7). Patchy areas of djerfisherite (2) have survived the decomposition process. When positioned near the original pyrrhotite-djerfisherite boundary the fine-grained pyrite and associated dark reflecting substance (5) have recrystallized into dense relatively coarse and homogeneous pyrite (8). The lamellae (3, 4 and 7) in the original unidentified dark reflecting substance (5) have survived this recrystallization process. (GGU 154130-A. × 525. Oil immersion).

alteration. Alternatively, the limonite formation (lamellae first, dense limonite later) may have taken place contemporaneously with the formation of respectively hematite-magnetite lamellae and interstitial fine-grained pyrite and unidentified dark reflecting substance. (d) Recrystallization of the fine-grained pyrite to relatively coarser pyrite (white, 8) may have taken place before the dense limonite formed and the pyrite crystals enclosed in the limonite have thus survived the limonite formation process. Alternatively, the pyrite is later than the limonite and has penetrated into it.

A rather similar situation is shown in fig. 14. Here the troilite has been altered into an extremely fine-grained, banded mixture of marcasite and limonite displaying bird's eye textures. The bands sweep concentrically around platy marcasite crystals which extend away
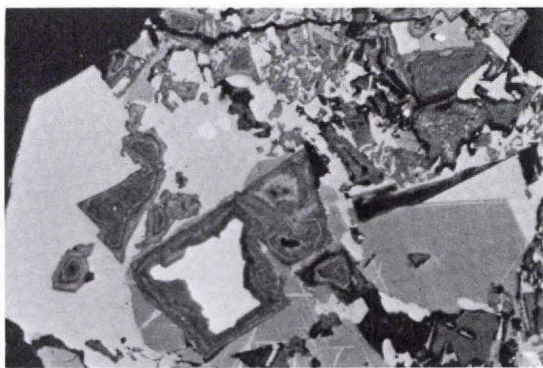

Fig. 15. Aggregate of subhedral magnetite (dark grey), hematite (light grey) and pyrite (white). The latter, originally isolated in both oxides, has been extensively replaced by limonite. (GGU 154327-4. ×485. Oil immersion).

from the original troilite boundary. Close to the same boundary, on the djerfisherite side, the fine-grained secondary pyrite and associated DRS (5), which originally developed between the lamellae of hematite (3) and magnetite (4), have recrystallized into almost pure pyrite (8). This process has not affected the earlier formed magnetite and hematite lamellae. The limonite lamellae (7) distinctly cut across both hematite and magnetite lamellae. At the upper right in the photographed area remnants of djerfisherite (2) have survived the alteration process.

Pyrite

A few pyrite grains were found in the green lujavrite (154359-1) and in the black kakortokite (154338-1). In the white kakortokite, aggregates of pyrite and magnetite (fig. 10) are considered to be decomposed troilite (described above). In the red kakortokite (154326-4), anhedral to euhedral pyrite is enclosed in aggregates of magnetite and hematite (fig. 15). All three minerals have been partly replaced by (? supergene) limonite.

Marcasite

Marcasite is a common supergene alteration mineral after troilite and pyrrhotite. Extremely rare marcasite has been found together with pyrite in lamellar intergrown magnetite and hematite in the white kakortokite (154327-4).

Molybdenite

Molybdenite occurs isolated in some of the Ilímaussaq rocks (fig. 4). It is generally not associated with other ore minerals. In 154352-29 (sodalite foyaite) it is intergrown with galena.

Chalcopyrite

Very sparse chalcopyrite has been found enclosed in one aggregate of pyrite and magnetite in the white kakortokite (154327-4). Sphalerite in the same polished section contains rare exsolved chalcopyrite. In the black kakortokite (154338-2), one magnetite grain contains a few blebs of chalcopyrite and pyrite. In the augite syenite chalcopyrite occurs as patchy grains in contact with troilite which contains exsolved 5.63C-pyrrhotite.

Loellingite

Two varieties of loellingite have been identified. One is primary while the other has developed during replacement of westerveldite. The primary variety is described here and the secondary variety below together with westerveldite.

Primary loellingite is generally shaped as prismatic crystals elongated parallel to the c axis. They may reach a length of 2 mm and they are up to 0.3 mm in cross section. The mineral is common in the white kakortokite (154327-14) but rare in the naujaite (57041-1) and in the red kakortokite (154326-12) (fig. 4). It has not been found in contact with other ore

Table 6. Microprobe analyses on westerveldite, loellingite, seinäjokite and gudmundite

		A westerveldite 154327-14		B loellingite 154327-14		C loellingite 154724-33	D seinäjokite 154724-31 and -33		E gudmundite 154724-31	
Number of grains analyzed		7		9		1	10		3	
wt. %	Fe	42.23	0.29	26.69	0.26	25.65	17.41	0.30	24.76	0.59
& esd	Co	0.38	0.02	0.92	0.24	0.40	0.33	0.21	0.07	0.07
	Ni	0.12	0.02	0.15	0.01	0.15	0.28	0.02	0.22	0.01
	As	55.48	0.31	70.91	0.50	63.79	1.75	0.44	0.45	0.33
	Sb	-		-		5.86	81.45	0.65	60.41	0.36
	S	0.35	0.15	0.50	0.16	0.49	0.08	0.01	14.52	0.28
		98.56		99.17		96.34	101.30		100.43	
Molar ratio	Fe	0.992		0.983		0.996	0.920		0.948	
	Co	0.008		0.032		0.015	0.017		0.003	
	Ni	0.003		0.005		0.006	0.014		0.008	
	As	0.982		1.948		1.846	0.069		0.013	
	Sb	-		-		0.104	1.973		0.968	
	S	0.014		0.032		0.033	0.007		1.061	
		1.999		3.000		3.000	3.000		3.001	

esd estimated standard deviation.

minerals. Microprobe analyses on loellingite from the white kakortokite are listed in Table 6 B. Guinier powder data (film no. 1604) and combined Weissenberg and precession studies gave *a* 5.260 ± 0.010 Å, *b* 5.980 ± 0.012 Å and *c* 2.940 ± 0.015 Å.

In the lujavrite MC (154724-33) rare platy loellingite crystals lie enclosed in seinäjokite (fig. 17). One microprobe analysis of poor quality due to the small crystal size, is listed in Table 6 C. It shows that the mineral contains considerable amounts of Sb. Loellingite from the Fe-Ni-As-Sb paragenesis at the Igdlúnguaq peninsula contains up to 5.05 per cent Sb (Oen *et al.* 1977).

Westerveldite and secondary loellingite

Westerveldite is a relatively common mineral in the white kakortokite, while only a few grains have been found in the red kakortokite, the sodalite foyaite and the naujaite. The mineral is generally replaced along the margins by loellingite (fig. 16), also when associated with galena. These relationships are identical with those between the same two minerals from pegmatites and hydrothermal veins within the intrusion (Karup-Møller & Makovicky,

Fig. 16. Westerveldite (1) is partly replaced by loellingite (2). The latter mineral is separated from the silicate minerals by a rim of magnetite, which, however, cannot be recognized in the photograph. The contact between the magnetite and the silicate minerals is stippled. (GGU 154327-4. × 95. Oil immersion).
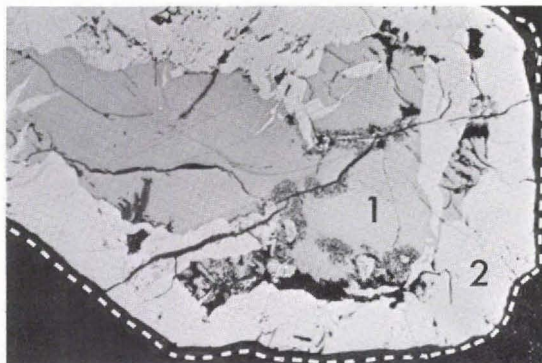
1977). The aggregate shown in fig. 16 and another aggregate of pure loellingite, presumably secondary after westerveldite in the same polished section, are separated from the silicate minerals by a narrow rim of magnetite.

Microprobe analysis on westerveldite in 154327-14 from the white kakortokite are listed in Table 6 A. The mineral contains, as westerveldite at locality A (fig. 1), small amounts of Co, Ni and S (Karup-Møller & Makovicky, 1977).

Seinäjokite

Seinäjokite ($FeSb_2$) has recently been described as a new mineral species (Mozgova *et al.* 1976) from Finland. Seinäjokite has been found in lujavrite MC from Kvanefjeld.

About 25 monomineralic seinäjokite grains were found in 154724-31 and 154724–33. A few grains contain regularly distributed blebs of an unidentified, exsolved mineral. Some of these grains also contain randomly oriented loellingite laths (fig. 17). Alteration (? supergene) of seinäjokite has sometimes taken place. The exsolved mineral and the loellingite laths have resisted alteration and they now lie isolated in a secondary, unidentified alteration product (fig. 17).

Optically, seinäjokite very closely resembles the gudmundite present in 154724-31. The

Fig. 17. Seinäjokite containing an exsolved, veryfine-grained, irregularly shaped, unidentified mineral. Partial (supergene?) alteration of the seinäjokite (right and upper left part in photograph) has taken place. The exsolved mineral and a platy loellingite crystal in the original seinäjokite have resisted this alteration process and now lie isolated in the secondary mineral. (GGU 154724-33. Nicols partly crossed). (× 750. Oil immersion).

Table 7. Reflectance data in air on
seinäjokite

λn	481	546	590	644
Rg	57.1	56.7	56.7	55.8
Rp	56.2	56.2	56.2	55.6

Instrument: Leitz-MPV. Standard SiC.
GGU sample no. 154724-33.

reflectance colour of seinäjokite is white with a distinct cream tint, especially in oil. The reflectance values recorded on one grain, showing maximum anisotropism under crossed nicols, are listed in Table 7. No reflectance pleochroism is visible. The anisotropism under crossed nicols is distinct to strong in air, strong in oil. The polarisation colours are vivid, red, reddish-brown, blue, violet and black. A few grains show irregular twinning. The micro-indentation hardness recorded in four points within one grain ranged from 412 to 435, the average being 426 (VHN_{50g}).

Seinäjokite is orthorhombic. Sufficient amounts of material could not be isolated for Guinier powder examination. Gandolfi powder data, obtained on material from the same mineral grain from which a splinter was isolated for the single crystal studies, are listed in Table 8. The diffraction lines recorded closely match the corresponding lines for synthetic $FeSb_2$ listed on ASTM cards 3-0717 and 3-0718 and those for seinäjokite from the type locality. However, considerably more lines were recorded on the synthetic phase than on the natural species. One line which is common to both natural seinäjokite from the Ilímaussaq intrusion ($d_{hkl} = 2.368$, Table 8) and synthetic $FeSb_2$ ($d_{hkl} = 2.40$, ASTM, card no. 3-0717) cannot be properly indexed. On the ASTM card it is indexed as (022). The d_{hkl} value for the line calculated on the basis of this indexing is 2.170. The closest possible line is (102) with a calculated d_{hkl} value of 2.280.

The cell dimensions for the natural seinäjokite calculated from the powder lines in Table 8 using the REFBASE III programme (written by E. Leonardsen, Institute of Mineralogy, University of Copenhagen) are listed in Table 9 A. In Table 9 B cell dimensions for synthetic $FeSb_2$ have been calculated using the corresponding powder lines published on the ASTM cards 3–0717 and 3–0718. The cell dimensions listed on the cards are reproduced in Table 9 C. Those published for synthetic $FeSb_2$ by Rosenqvist (1954) are reproduced in Table 9 D, and those for seinäjokite from the type locality by Mozgova *et al.* (1976) are given in Table 9 E.

Microprobe analysis on 10 seinäjokite grains 154724–31 and 154724-33 are listed in Table 6 D and suggest the formula:

$(Fe_{0.92}Co_{0.02}Ni_{0.01})$ $(Sb_{1.97}As_{0.07}S_{0.01})$ or idealized $FeSb_2$.

The following composition was obtained for seinäjokite from the type locality:

$(Fe_{0.78}Ni_{0.20}Co_{0.03})$ $\Sigma_{1.01}(Sb_{1.71}As_{0.26}Te_{0.03})\Sigma_{2.06}$.

The fine grain size of the exsolved mineral which occurs in a few of the seinäjokite grains has excluded the recording of satisfactory microprobe analyses. A semi-quantitative analysis on the largest observed grain gave: 77 % Sb, 9 % Fe, 3 % Co, 1 % As, 0.3 % Ni and 0.1 % S

Table 8. X-ray powder data on seinäjokite

I	$d_{obs.}$	$d_{cal.}$	Indices
6	2.853	2.850	012
1	2.788	2.795	110
2	2.663	2.661	021
5	2.574	2.570	111
2	2.368	Indexing not possible	
8	2.047	2.042	121
1	1.861	1.862	031
10	1.799	1.798	103
2	1.660	1.658	130
4	1.228	1.228	142
3	1.213	1.211	043
1	1.184	1.184	115
3	1.164	1.164	134
2	1.130	1.322	143
6	1.065	1.062	224
3	0.889		
6	0.863		
2	0.855		
3	0.839		
1	0.823		
7	0.817		
8	0.811		
6	0.786		

Gandolfi camera. Cu-rad. Film no. 159.
GGU sample no. 154724-31.

with a sum of only 90 %. The poor analysis suggests a composition rather close to that of the host. The optical properties are close to those of seinäjokite.

The analysis of one loellingite lath originally enclosed in seinäjokite (lower middle-left in fig. 17) is listed in Table 6 C. The content of Sb in this mineral variety is 5.89 %. The content of As in the seinäjokite is 1.75 % (Table 6 D). The recorded values thus give some indications of the solubility of As and Sb in seinäjokite and loellingite respectively, when these two minerals coexist.

The relationships between synthetic seinäjokite and other phases in the system Fe–Sb–S are described by Barton (1971).

Gudmundite

A few monomineralic gudmundite grains (identified on the basis of microprobe analyses and optic study only) occur in lujavrite MC (154724-31). Microprobe analyses on three grains are listed in Table 6 E. According to Barton (1971), gudmundite is stable only at

Table 9. Cell dimensions for seinäjokite

	A	B	C	D	E
a =	3.185±0.009	3.189±0.003	3.189	3.204	3.19±0.01 Å
b =	5.827±0.006	5.810±0.006	5.819	5.83	5.81±0.01 Å
c =	6.536±0.005	6.524±0.006	6.520	6.55	6.49±0.015 Å

A: Present study. GGU sample no. 154724-31. B: Calculated on basis of powder data from ASTM cards 3-0717 and 3-0718. C: Cell dimensions listed on the ASTM cards. D: Cell dimensions published by Rosenqvist (1954) and E: Cell dimensions published by Mozgova *et al.* (1976).

temperatures below 280°C. This would imply crystallization of the lujavrite MC magma down to temperatures below 280°C, which appears very unlikely. Alternatively, the mineral may either have formed by recrystallization or it has crystallized under hydrothermal conditions in mineral pockets within the lujavrite MC.

Gudmundite from the Ilímaussaq intrusion has previously been found only in the Igdlúnguaq Ni-Fe-As-Sb association (Oen & Sørensen, 1964; Oen *et al.*, 1977).

Native tin, native lead and unnamed Sn-Cu(-Pb) phase

In the white kakortokite (154327-14) one single aggregate was found to be composed of extremely fine-grained granular native tin with interstitial native lead. Numerous crystals of an unnamed Sn-Cu(Pb) phase (fig. 18) are enclosed in the native tin. Five similar aggregates of native tin and lead but without the unnamed Sn-Cu(-Pb) mineral were found in the red kakortokite (154326-12) and a further aggregate in the black kakortokite (154338-1a). The possibility that the aggregates with native tin represent contaminating material cannot be excluded although they have been found in all three kakortokite varieties. They have therefore not been considered in the discussion below on the conditions of formation of the ore minerals.

Microprobe analyses on the *native lead* gave 2.5 wt. per cent (4.3 atomic per cent) Sn and 0.4 wt. per cent (1.3 atomic per cent) Cu. The only two phases known in the Pb–Sn system
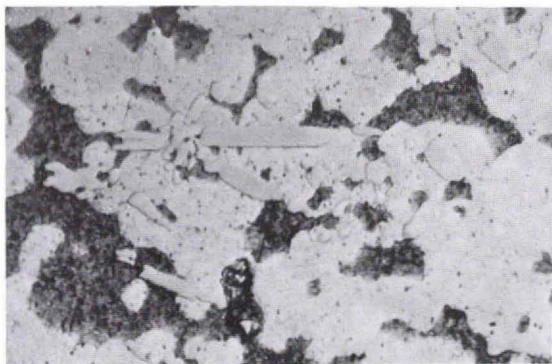

Fig. 18. Aggregates of granular, native tin (white) with intergranular native lead (black due to poor polish and tarnish) contain lamellae of unnamed Sn-Cu(-Pb)mineral. (GGU 154327-14). × 1270. Oil immersion).

Table 10. Microprobe analyses on unnamed Sn-Cu(-Pb) mineral

	Wt. %	Molar ratio	Wt. %	Molar ratio	Wt. %	Molar ratio
Sn	48.6	37.1	50.7	38.3	48.4	34.4
Cu	42.0	60.0	39.9	56.3	45.2	60.1
Pb	6.7	2.9	12.5	5.4	1.5	0.6
	97.4	100.0	103.1	100.0	95.1	100.1

Analyses on three grains in sample GGU 154327-14.

are lead and tin (Hansen & Anderko, 1958). At about 180°C they crystallize in eutectic intergrowth. At these temperatures, lead may contain up to 28 atomic per cent Sn. At room temperatures the maximum Sn content is 3.4 atomic per cent, while that of Cu is negligible.

Microprobe analyses on the *native Sn* gave 0.7 wt. per cent Pb and 0.1 wt. per cent Cu. According to Hansen & Anderko (1958) native tin in the system Sn–Pb may contain around 1.5 to 2.6 wt. per cent Pb at the eutectic temperature ($\sim$ 180°C), while in the system Sn–Cu its maximum content of copper at temperatures below 232°C is around 0.001 per cent.

The unnamed Sn-Cu(-Pb) phase lies at random in the native tin. Occasionally it penetrates into the native lead. The crystals are subhedral to euhedral and platy in shape (fig. 18). The optical properties vary. Relatively 'large' crystals have a distinct violet reflectance colour. The reflectivity is near that of the host native tin. Reflectance pleochroism is not visible. Anisotropism under crossed nicols is strong but the anisotropism colours are not distinct. Smaller crystals and the marginal areas of the larger crystals lack the pronounced violet colour. They are cream white with a slight pinkish tint. The anisotropism under crossed nicols appears less pronounced than that of the violet coloured grains. Both varieties display oblique extinction and their hardness is distinctly higher than that of the host tin. It cannot be excluded that two phases are present and the violet coloured variety is replaced by the cream pinkish coloured. Reliable microprobe analyses could not be obtained on crystals of the latter variety due to its small size. Acceptable microprobe analyses were completed on three crystals of the violet variety (Table 10). No natural or synthetic phase with compositions corresponding to that of the violet coloured mineral are known to the author. Simple substitution in the mineral of lead for either copper or tin does not yield compositions which resemble those of any synthetic phases known in the system Sn–Cu (Hansen & Anderko, 1958).

Only two tin-bearing minerals from the Ilímaussaq intrusion have been described, stannite by Oen & Sørensen (1964) and the beryllium-bearing silicate sorensenite with about 18 % Sn by Semenov *et al.* (1965).

Native iron and wüstite

Steel flakes from the rock crusher are present in all hand magnetic fractions. Generally these grains are easily identified due to their characteristically deformed shape.
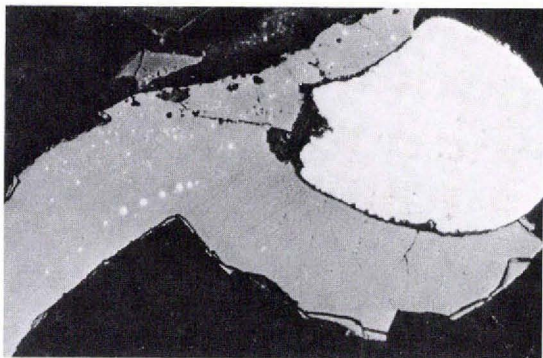
Fig. 19. Oval-shaped native iron with small cavities is partly enclosed in magnetite disseminated with spheroidal circles of native iron. (GGU 154724-1. × 570. Oil immersion.)

In 154724–1 from lujavrite MC rounded, often perfectly circular, iron spheres less than 0.5 mm in diameter, are enclosed in dendritic magnetite (fig. 19). The native iron contains small cavities.

Fine-grained intergrowths between magnetite and very fine-grained native iron were identified in the ore mineral concentrates from the white and red kakortokites. These intergrowths are considered to be the decomposition products of 'wüstite'.

In polished sections welding pearls and fragments display similar textural relations between magnetite and native iron as shown in fig. 19. The native iron and associated magnetite in the heavy mineral fractions are therefore at present assumed to represent contaminating material. Intergrowth between these ore minerals and silicate minerals from the Ilímaussaq intrusions, if ever found, will correct this assumption.

## Magnetite, hematite, ilmenite, chromite, ulvöspinel and rutile

Magnetite and hematite occur as accessory minerals in several of the Ilímaussaq rocks (fig. 4).

Aggregates of magnetite and hematite from the red kakortokite (154326-4) contain idiomorphic pyrite (fig. 15). Alteration of arfvedsonite in this rock is accompanied by the crystallization of magnetite, hematite and rutile along cleavage directions. Similar materials have also been observed in 154352-18 from the sodalite foyaite. Aggregates of magnetite and hematite similar to those shown in fig. 15, but without pyrite may gradually extend into the partly altered arfvedsonite. Therefore, alteration of the arfvedsonite and formation of the magnetite-hematite-(pyrite) aggregates are considered to be genetically related.

A few grains of chromite in 154338-2 from the black kakortokite have been identified by microprobe. They are all partly replaced by magnetite. The possibility that this chromite represents contamination from earlier material crushed and separated in the laboratories cannot be excluded.

In the heavy mineral concentrate (154352-2) from the sodalite foyaite, rounded aggregates of a generally very fine grained decomposition intergrowth of magnetite and ilmenite have been identified (fig. 20). A relatively large proportion of silicate minerals has crystallized in the marginal areas of the aggregates. The oval to circular shape of the aggregates suggests crystallization from an immiscible oxide phase.

Fig. 20. Rounded aggregate of finely intergrown magnetite, ilmenite and in the marginal areas silicate minerals. The two oxides are secondary after a former high temperature phase. (GGU 154352-2. × 285. Oil immersion).
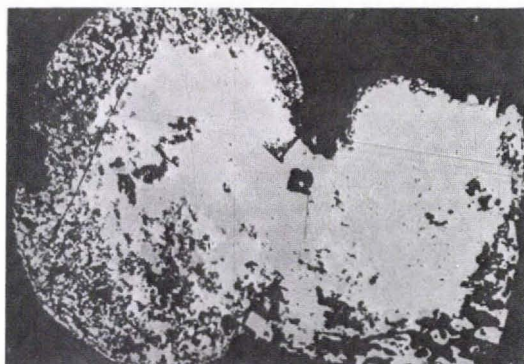
In the augite syenite, decomposition aggregates composed of extremely fine-grained intergrown ilmenite and ulvöspinel in all proportions are common (154332-5). Exsolution lamellae of hematite from the original high temperature phase are preserved in the decomposition products.

The alkali granite contains abundant ilmenite but only sparse magnetite (154379-34 and 154379-35). Secondary hematite and rutile are also present. Exsolution-decomposition intergrowths have not been observed.

Comparison between the accessory rock-forming ore minerals and the ore minerals in pegmatites and pneumatolytic-hydrothermal veins

Pronounced similarities and differences exist between the types of accessory ore minerals in the major rock types and the ore minerals found in pegmatites and pneumatolytic-hydrothermal veins.

The ore minerals belonging to association I (Pb-Zn-Mo) and association III (Fe-As) are relatively common in the veins and in the major rocks. Both associations are made up of the same species (galena, native lead, sphalerite, molybdenite, westerveldite and loellingite) which display similar relationships. Cu-Sb-bearing minerals (sulphides, oxides, native elements and alloys) and pure Cu-sulphides (association II) have not been found in the rocks. They are very characteristic for the vein ore mineralogy. The only accessory rock forming ore minerals belonging to association IV are gudmundite and seinäjokite. They occur in sparse amounts only in the lujavrite MC. The vein ore minerals belonging to the same association are likewise rare, being known only from locality 7 in fig. 1.

Age relationships between accessory ore minerals and host silicate minerals in the major rocks

Age relationships between accessory ore minerals and host silicate minerals could not be studied in the heavy mineral concentrate except for a very few cases. However, they can to a certain degree be estimated indirectly.

Ussing (1912) considers the layering of the kakortokites to be the result of variation in vapour pressure. This variation may have been caused by repeated volcanic explosions on the surface. However, experimental results by Piotrowski & Edgar (1970) do not indicate any change in the order of separation of the cumulus minerals caused by variation in vapour pressure. Accordingly Sørensen (1969) favours intermittant, penecontemporaneous crystallization of the cumulus minerals. Differential settling of these would explain the mineral-graded three-layered sequence. The distribution of the ore minerals, few in the black kakortokite and abundant in the red and white kakortokites, suggests that they crystallized at a late stage from an intercumulus liquid phase present in larger amounts in the white and red than in the black kakortokite layers.

At vein locality A in fig. 1 similar age relationships exist between silicate minerals, arsenides and sulphides. Here analcime and ore minerals (westerveldite, loellingite, sphalerite, galena and molybdenite) have crystallized interstitially to the early nepheline and idiomorphic eudialyte. Observations at other localities suggest penecontemporaneous crystallization of similar veins (without ore minerals) and black lujavrite. The temperatures of formation of the ore minerals might therefore have been at least 400°C (Karup-Møller & Makovicky, 1977).

The highest content of troilite has been found in the naujaite. In this rock arfvedsonite crystallized late. The content of iron in the rest magma must therefore have gradually increased and thus promoted the formation of pyrrhotite and djerfisherite. In the kakortokite an early arfvedsonite formation may be responsible for the relatively small contents of troilite-djerfisherite in these rocks.

The green lujavrites and the lujavrite MC does not contain troilite/pyrrhotite and djerfisherite. Heavy mineral concentrates have not been isolated from the black lujavrite, but no iron sulphides have been identified during microscopic and macroscopic examinations of this rock type. In the lujavrites arfvedsonite appears both to be cumulus and intercumulus (sometimes poikilitic) while aegirine is a cumulus phase (Engell, 1973). The crystallization of arfvedsonite and aegirine does not therefore appear to have played any decisive role in preventing the formation of Fe-sulphides. The abundance of PbS and the absence of native lead (except in lujavrite MC) indicates that the absence of troilite cannot be explained by sulphur fugacities below the FeS-Fe boundary (fig. 21).

Pyrrhotite/troilite and djerfisherite have not been found in the pegmatites and pneumatolytic-hydrothermal veins. This is in spite of the fact that galena, sphalerite and molybdenite are fairly common, as they are in the naujaite where they are

Table 11. Average content (ppm) of selected elements in the Ilímaussaq intrusion,
the Lovozero massif and in acid, basic and ultrabasic rocks

	Ilímaussaq	Lovozero	Acid	Basic	Ultra-basic
Fe	70300	42360	27000	85600	98500
Ti	2070	6700	2300	900	300
F	2100	1400	800	370	100
Cl	8800	1600	240	50	50
S	910	1020	400	300	100
Zn	870	210	60	130	30
Pb	225	14.6	20	8	0.1
Sn	115	10	3	1.5	0.5
Mo	14	1.7	1	1.4	0.2
Tl	3.1	0.86	1.5	0.2	1.01

Reproduced from Gerasimovsky, 1969, table 12.

associated with the two Fe-sulphides. Iron is present in substantial amounts in the late hydrothermal veins. Possibly (as just argued) early crystallization of Fe-silicates may substantially have depleated the vein material of iron thus preventing the formation of pyrrhotite/troilite and djerfisherite.

In *conclusion,* the few observations on the relationships between sulphides and silicate minerals in the Ilímaussaq agpaitic rocks suggest that sulphides and arsenides crystallized late compared with the silicate minerals. In the augite syenite, pyrrhotite crystallized from immiscible droplets enclosed in olivine and possibly also in other silicate minerals.

Bulk chemical composition of the major Ilímaussaq rocks and their bearing upon the crystallization of the ore minerals

The chemical compositions of samples representing each of the major Ilímaussaq rock types have been published by Gerasimovsky (1969). Limited chemical investigations on rocks in the northern part of the intrusion were carried out by Hamilton (1964). Ferguson (1970) has undertaken detailed chemical studies of the kakortokites in the southern part of the intrusion. Preliminary results for some elements relevant to the present study have recently been completed on samples from the uppermost layered kakortokites by J. Bailey (personal communication).

At present a detailed chemical study of the characteristic rocks and major minerals from the Ilímaussaq intrusion is in progress at the Institute of Petrology, University of Copenhagen. The results of this study may eventually allow more detailed conclusions about the distribution of trace elements among ore and silicate minerals than those possible at present.

The average contents of elements in the Ilímaussaq intrusion and the closely related Lovozero intrusion in the USSR, which are considered important for the present study, are listed in Table 11. The table also includes the average content of acid, basic and ultrabasic rocks. For detailed analytical results on individual rock types the reader is referred to the paper by Gerasimovsky (1969). Unfortunately the data for several elements critical to the present study are incomplete (Ni, Co, Cu, Cr, As, Sb and Ag).

Compared to common rocks the contents of Cl, Zn, Pb, Mo and Sn in the agpaitic rocks of the Ilímaussaq intrusion are exceptionally high, while those of F, S and Tl are enriched by a factor of two or more. All these elements are also (except for S) remarkably higher in the Ilímaussaq intrusion than in the Lovozero massif. Great differences exist among the individual agpaitic rock types of the Ilímaussaq intrusion as to the content of most of these elements, especially Cl. The content of Cl in the naujaites is 2.4 per cent while in the other rocks it ranges between 3200 and 3000 ppm. The rather uniform content of sulphur in the Ilímaussaq rocks is characteristic. The contents of Ni (<5ppm), Co (<5ppm), Cu (<10 ppm) and Cr (<4ppm) recorded on kakortokite rocks by J. Bailey are exceptionally low; but those for As (5-10 ppm) are high compared to normal rocks. The Ag content in the kakortokite rocks is less than 2 ppm.

The amount of accessory ore minerals in the Ilímaussaq rocks is low considering the exceptionally high contents of certain trace elements when compared to normal rocks. This is due to the nature of agpaitic melts. Their capacity to dissolve and retain volatile components (H_2O, F, Cl, CO_2 and S) increases with rising alkalinity (Kogarko, 1974). Separation of volatiles is thus severely limited in agpaitic systems and may first take place at late stages of the crystallization when fields of silicate versus alkali halide liquid immiscibility may be reached (Kogarko *et al.*, 1974). On crystallization the volatiles to a large degree enter into the solid phases (sodalite-hackmanite, eudialyte, villiaumite, arfvedsonite and hydrous aluminosilicates). This is especially so in naujaites where sulphur and unusually large amounts of chlorine are contained in sodalite-hackmanite, with chlorine also in eudialyte. Consequently, the crystallization of sulphides is suppressed and the metals are fixed in the silicates.

The mineralized vein at locality A in fig. 1 is considered to be derived from re-mobilized naujaite (unpublished observations). The exceptionally high concentrations of westerveldite, loellingite, sphalerite, galena and molybdenite may represent the accumulation of ore elements from the mobilized accessory ore minerals in the naujaite. The presence of arsenides in pegmatites and pneumatolytic-hydrothermal veins at the other localities suggests the concentration of As in the post-magmatic fluids and its subsequent fixation as arsenides.

The incomplete analytical data on Cu, Ag and Sb in the rocks of the Ilímaussaq intrusion, exclude specific conclusions to be drawn about the distribution of these elements in the intrusion. This is unfortunate because distinct Cu-Sb-(Tl-Ag) ore

mineral associations (association II) are characteristic for the pneumatolytic-hydrothermal veins. Small amounts of seinäjokite ($FeSb_2$) and gudmundite (FeSbS) occur in the lujavrite MC and represent the only antimonides found as accessory rock-forming ore minerals. The Cu-Sb-(Tl-Ag) mineralization at locality 2 in fig. 1 occurs in a natrolite-sodalite vein along the contact between lujavrite MC and a trachyte dyke. The vein material is considered to be a late magmatic phase of the lujavrite MC formation (Karup-Møller, 1978). It is therefore assumed that at least within the Kvanefjeld area the late magmatic melts and fluids have been enriched in the elements Cu, Sb, Tl and Ag as the consolidation of the Ilímaussaq intrusion came to a conclusion.

The distribution of the Fe(Cu) sulphides in the naujaites and in the kakortokites is essentially considered to be a function of the crystallization sequence of the silicate minerals, mainly arfvedsonite and aegirine (discussed earlier).

The Cu-Sb, Fe-As and Fe-Ni-As-Sb ore mineral associations are sharply separated from each other at all localities. No zonality was observed, although different associations may occur relatively close to each other. However, the number of occurrences may not be sufficiently large to support the universality of this observation. The sharp separation of the ore mineral associations may have resulted from separation of the ore mineral components at different levels and moments during the consolidation of the parent lujavrite magma. Different fS_2 and fO_2 levels but also different chemical bulk compositions (fig. 2) explain the different mineralogical compositions of the two Cu-Sb subtypes IIa and IIb at locality 2 in fig. 1.

SULPHUR AND OXYGEN FUGACITY CONDITIONS OF FORMATION

Crystallization of the ore minerals in rocks and veins at the Ilímaussaq intrusion is essentially a function of the prevailing sulphur and oxygen fugacities, temperatures and availability of metals.

Sulphur fugacity

Exceptionally low sulphur fugacities prevailed during the crystallization of the agpaitic rocks, pegmatites and mineral veins of the Ilímaussaq intrusion. This is due to the relatively late and limited separation of volatiles from agpaitic melts which caused the extensive fixation of sulphur in the silicate minerals (discussed above).

Log a_{S2} (logarithm of the sulphur fugacity) versus temperature for a number of characteristic ore mineral assemblages is shown in figs 21 and 22. The data in the two figures have been put together in close collaboration with E. Makovicky,
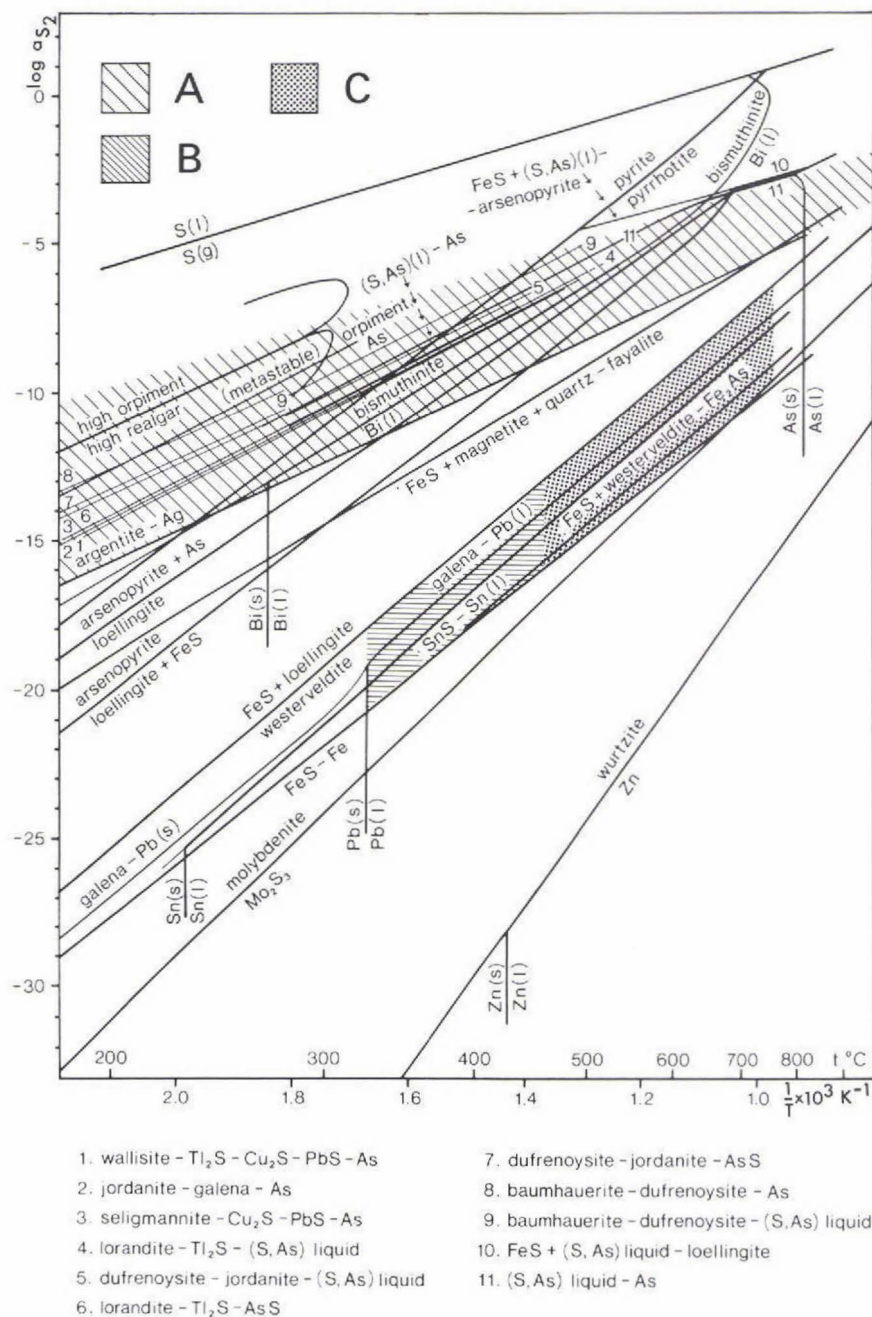
Fig. 21. Sulphidation equilibria for selected sulphides and arsenides based upon published thermodynamic data. A: 'Main-line' of ore mineral forming environments. B: Principal regimes for the Ilímaussaq ore minerals (mainly association III) in pegmatites and pneumatolytic-hydrothermal veins, and C: principle regimes for the ore minerals in some of the major agpaitic rocks. For details see text. 'FeS' stands for pyrrhotite compositions.

Institute of Mineralogy, University of Copenhagen. They are based upon thermo-dynamic data published by Barton & Skinner (1967), Barton (1969, 1971, 1973) and Craig & Barton (1973). On the basis of the two plots it is possible, semi-quan-titatively, to estimate the prevailing sulphur fugacities during the crystallization of the ore minerals from the Ilímaussaq intrusion. In Karup-Møller & Makovicky (1977) the particular conditions controlling the crystallization of the minerals be-longing to the Fe-As association have been discussed.

Accessory rock-forming ore minerals

The Ilímaussaq agpaitic rocks are assumed to have crystallized at temperatures between 900°C and 450°C (e.g. Sørensen, 1969), the lujavrites even at tempera-tures as low as 400°C (Piotrowsky & Edgar, 1970). It has been concluded earlier that most of the accessory ore minerals have crystallized late in relation to the major rock-forming silicate minerals, possibly in the temperature interval of 700°C and 450°C. Exceptions to this are native lead which melts at 327°C at a pressure of one atmosphere. Part of the galena associated with the native lead may have crystallized at temperatures close to 327°C. Gudmundite, stable only at tempera-tures below 280°C (Barton, 1971), may either have formed by recrystallization or it may have crystallized at lower temperatures in hitherto undetected mineral pockets in the host.

In the 700°C and 450°C temperature region ore mineral associations identified suggest sulphur fugacities corresponding to area C in fig. 21. The maximum $\log a_{S2}$ values at the two temperature limits are ~-6.5 and ~-12.9 and the minimum values ~-9.7 and ~-15.0.

Molybdenite. The absence of Mo_2S_3 in the presence of MoS_2 in the rocks, peg-matites and pneumatolytic-hydrothermal veins (ore microscope examinations on-ly) place the general minimum sulphur fugacity at which both rock and vein ore minerals crystallized above the line Mo_2S_3 - MoS_2 in fig. 21.

Westerveldite-loellingite. Primary westerveldite and loellingite have crystallized in white and red kakortokite, naujaite and sodalite foyaite.

The stability of westerveldite and loellingite is a function of both the arsenic-fu-gacity and the sulphur-fugacity. The existence of westerveldite suggests sulphur fugacities below the FeS + loellingite – westerveldite line in fig. 21. The sulphur fugacity at which the primary loellingite crystallized cannot be estimated.

Westerveldite in Ilímaussaq is partly replaced by loellingite and as a result iron was set free: $2FeAs \rightarrow FeAs_2 + Fe$. This decomposition process may very well be post-magmatic in origin. Oxidation of freed iron may explain the magnetite rim surrounding westerveldite-loellingite aggregates (fig. 16).

In the naujaite and sodalite foyaite numerous grains of westerveldite replaced by loellingite are not associated with magnetite or pyrrhotite. In these rocks iron set free was therefore separated from the two arsenides and concentrated elsewhere,
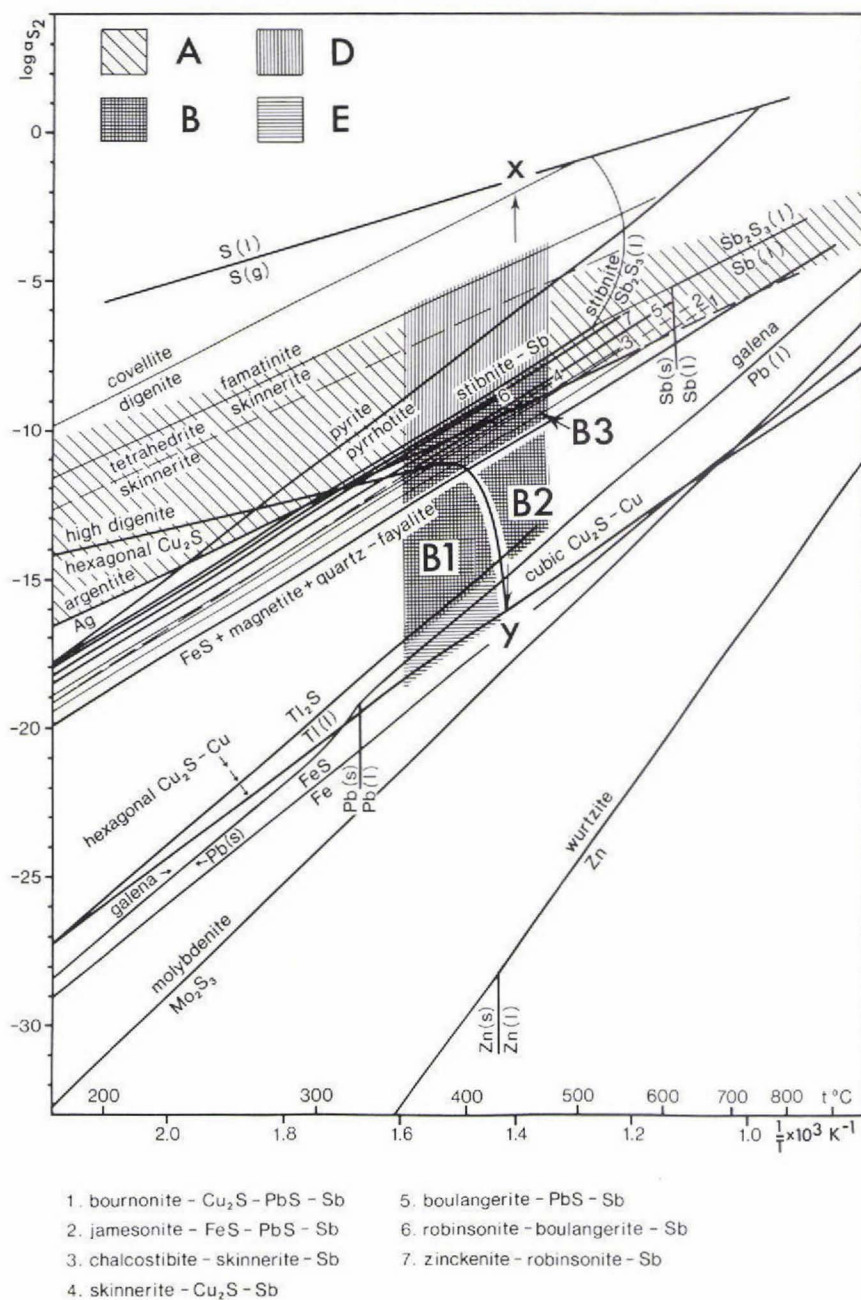
Fig. 22. Sulphidation equilibria for selected sulphides and antimonides based upon published thermodynamic data. A as in fig. 21. B1-B3 principal regimes for the ore minerals (mainly association II) in pegmatites and pneumatolytic-hydrothermal veins. D and E possible extension of area B. For details see text. 'FeS' stands for pyrrhotite compositions.

either in silicate minerals or in pyrrhotite. Sulphur for the possible pyrrhotite formation could have been supplied from sulphur dissolved in the silicate minerals, preferably sodalite. If the freed iron was bound in pyrrhotite, then the sulphur fugacity would have been above the FeS + loellingite–westerveldite line in fig. 21. If pyrrhotite did not form then the sulphur fugacity may have been below the line.

A characteristic feature is the complete absence of arsenopyrite from the Ilímaussaq intrusion. The sulphur fugacity which prevailed during the crystallization of the arsenides therefore apparently never reached the arsenopyrite-loellingite + FeS line in fig. 21.

Galena-native lead. The association galena–native lead occurs in the lujavrite MC and suggests sulphur fugacities distinctly below the FeS + loellingite–westerveldite line in fig. 21. The consistent presence of galena and not native lead associated with westerveldite in the rocks from the Ilímaussaq intrusion confirms the position of the galena - Pb line below the FeS_2 + loellingite–westerveldite line.

Seinäjokite. The line $FeSb_2$ (seinäjokite)–pyrrhotite + native antimony in the log a_{S2} versus temperature plot has been determined by Barton (1971, fig. 4). The line is not shown in fig. 21 but would, at temperatures below ~720°C, have lain between the line FeS + loellingite–westerveldite and the line galena–Pb(l). Seinäjokite thus crystallized at low sulphur fugacities similar to the association galena - native lead present also in the lujavrite MC.

Troilite-pyrrhotite. Perhaps the most significant mineral for the sulphur fugacity estimates is the Ilímaussaq high temperature, disordered hexagonal pyrrhotite (1C). It has crystallized in several of the Ilímaussaq rock types (fig. 4). At temperatures above ~140°C the Fe content of this sulphide may range from approximately 48 to exactly 50 mol. per cent Fe. The sulphide is unquenchable, and varieties of intermediate composition decompose to a mixture of troilite and pyrrhotite. The latter is characterized by one of several superstructure possibilities.

In the sodalite foyaite, the naujaite and the white kakortokite the composition of the hexagonal pyrrhotite (1C) is stoichiometric FeS. At decreasing temperatures, around 140°C, it therefore recrystallized to pure, monomineralic troilite. In the augite syenite the troilite contains exsolved pyrrhotite (5.63C) in the visually estimated proportion 3:1. This corresponds to a composition of approximately $Fe_{0.99}S_{1.01}$ for the original hexagonal pyrrhotite (1C).

The composition of the pyrrhotite (1C) in the pure FeS system is a function of temperature and sulphur fugacity (e.g. Craig & Scott, 1974, fig. CS-8). The FeS–Fe and the pyrrhotite–pyrite stability lines are plotted in figs 21 and 22. The line for pyrrhotite with a composition corresponding to that estimated for the original pyrrhotite (1C) in the augite syenite would plot in both figures at approximately half a centimetre above the FeS–line.

The augite syenite pyrrhotite occurs as immiscibility droplets in the silicate minerals, e.g. in olivine. It must therefore have crystallized at a relatively high temperature. A similar habit for troilite in the agpaitic nepheline syenites has not been

observed. In these rocks the sulphide is assumed (see discussion above) to have crystallized relatively late in relation to the major rock-forming silicate minerals. An early crystallization of pyrrhotite (1C) in the augite syenite might have taken place at temperatures well above 700°C, which excludes reasonable sulphur fugacity estimates.

Troilite is the dominant phase in the decomposed pyrrhotite from the augite syenite. This shows that the original sulphide must have crystallized under sulphur fugacity conditions considerably lower than those prevailing during the crystallization of pyrrhotite in 'normal' sulphide deposits. However, compared to the conditions in the agpaitic rocks of the Ilímaussaq intrusion the sulphur fugacity must have been higher.

The troilite (FeS) composition of the original pyrrhotite (1C) in all agpaitic nepheline syenites is at variance with the calculations of Kogarko (1972) which are based on the assumption that the a_{S2} values for the agpaitic magmas are controlled by the pyrrhotite/FeS_2 buffer. This hypothesis rests on the formation of pyrite within the Lovozero intrusion. The mineralogy of the ore minerals of this intrusion is restricted to a few of the common sulphides and arsenides. Detailed crystallographic examination of the Lovozero pyrrhotite has apparently not been carried out (Semenov, 1972)

Sphalerite. The Fe content in sphalerite which has crystallized in equilibrium with pyrrhotite is a function of the pyrrhotite composition and the *P–T* conditions of formation (e.g. Craig & Scott, 1974, figs CS-13 and CS-15). Sphalerite has been found in smooth contact with troilite in the naujaite (57041-2), which suggests that the two sulphides formed in equilibrium. The naujaite sphalerite contains from 9.6-14.1 per cent Fe (Table 3). Some of the analyzed grains have crystallized in contact with pyrrhotite. The iron content in sphalerite from other agpaitic rock types ranges between 0.3 and 14.5 per cent. According to Sørensen (1969) the Ilímaussaq intrusion has probably consolidated at a depth in the crust corresponding to a load pressure of approximately 0.5-1.5 kb. The vapour pressure is assumed to have been significantly higher, in the range 1-3 kb. Under these conditions and assuming a temperature of between 700°C and 450° C, the sphalerite in equilibrium with troilite should, according to Craig & Scott (1974), contain about 43 mol. per cent FeS. This is considerably more than recorded on the naujaite sphalerite.

Troilite-djerfisherite. This mineral association occurs in the naujaite, the sodalite foyaite and the white kakortokite. Djerfisherite was first found associated with troilite in chondritic meteorites. The combination of low sulphur fugacity and small contents of Cu and K in the Cl-rich agpaitic magmas explain the crystallization of the djerfisherite. The corresponding mineral association in the augite syenite and in 'normal' sulphide deposits is probably pyrrhotite-chalcopyrite.

Chalcopyrite. Extremely small amounts of chalcopyrite have crystallized when the hypogene secondary pyrite-magnetite aggregates developed in the white kakortokite. Sphalerite in the same rock contains minute exsolved chalcopyrite.

Pyrite. The significance of the very few grains of monomineralic pyrite found in the green lujavrite, the black kakortokite, the sodalite foyaite and the alkali granite is difficult to estimate. If primary, their presence suggests sudden, possibly local and short-lived, increases in the sulphur fugacity to and above the pyrrhotite–pyrite line (fig. 22). This at least explains the formation of pyrite in the late or post-magmatic hypogene magnetite-hematite-pyrite aggregates (figs 10 and 15) found in kakortokite.

Ore minerals in pegmatites and veins

The vein ore minerals are considered to have crystallized within the temperature range of 450°-350°C. This estimate is based on the thermal stability of several minerals and mineral assemblages. Native lead melts at 327° C. Skinnerite is stable at temperatures between 359° and 607°C; the upper temperature limit of pure tetrahedrite is 543°C, for cuprostibite it is 586°C and for the tetrahedrite-skinnerite-Sb association 436°C, all in the condensed system (Skinner *et al.*, 1972). The lujavrites are assumed to have crystallized at temperatures down to 450°–400°C (Piotrowsky & Edgar, 1970; Sørensen, 1969).

The pneumatolytic-hydrothermal mineral veins are considered to have crystallized from late magmatic fluids expelled from the lujavrite magma when it consolidated. Occasionally vein materials have been mixed with lujavrite in fractures cutting huge naujaite inclusions in the lujavrite (e.g. at the peninsula exactly two and a half kilometres directly north of locality 4 in fig. 1). This would imply crystallization temperatures for the vein materials of up to approximately 450°C.

Ore minerals belonging to the *associations I (Pb-Zn-Mo)* and *III (Fe-As)* are present in the pegmatites and pneumatolytic veins. They are the same as those identified in the rocks and they display similar relationships. The fugacity conditions under which the vein ore minerals in the Fe-As association crystallized have been discussed in detail by Karup-Møller & Makovicky (1977). The estimated sulphur fugacity range between 350°C and 450°C is represented by area B in fig. 21. At 400°C the estimated log a_{S2} ranges from ~–17.9 to –15.0.

The apparent absence of Mo_2S_3 places the minimum sulphur fugacity ranges above the line molybdenite – Mo_2S_3 in fig . 21.

The absence of arsenopyrite indicates that the fugacity never reached the arsenopyrite–loellingite + FeS line. Also, the presence of native antimony crystals in the galena associated with westerveldite partly replaced by loellingite (Karup-Møller & Makovicky, 1977, fig. 19) indicates sulphur fugacity values below the jamesonite – FeS + PbS + Sb line (no. 2 in fig. 22).

The ore minerals (including Ni-westerveldite) which belong to the *Fe-Ni-As-Sb association* (from locality 7 in fig. 1) presumably crystallized under sulphur fugacities similar to those under which the minerals belonging to associations I and III formed.

Association II (Cu-Sb) contains two subtypes, (a) the (Cu-Sb) subtype and (b) the Cu-Sb-S subtype.

Cu-Sb subtype (IIA). Unfortunately, the fugacity values for the sulphidation of Cu_2Sb have not been determined. The presence of chalcocite, antimonian silver, galena and loellingite, against the absence of digenite, argentite, native lead and westerveldite in the cuprostibite lumps at localities 2a and 3 in fig. 1, suggests fugacities corresponding to the area B1 in fig. 22. At 400°C the estimated log a_{S2} range is ~–15.6 to ~–11.8.

At locality 2a extremely sparse native copper occurs in dyscrasite (Karup-Møller, 1978) which suggests sulphur fugacity conditions corresponding to area E in fig. 22.

Traces of hypogene, primary argentite and chalcopyrite in cuprostibite at locality 1 in fig. 1 were described by Sørensen *et al.* (1969b). The crystallization of argentite (and presumably also chalcopyrite) in association with cuprostibite appears to be at variance with the sulphur fugacity stability range of cuprostibite.

Both rohaite and chalcothallite represent complex sulphur-poor sulphides of mainly Cu, Sb and Tl. Their stability is in accordance with the low sulphur fugacity conditions for the Cu_2Sb veins.

The composition of high digenite at 435°C ranges between $Cu_{1.76}S$ and $Cu_{2.00}S$ (Roseboom, 1966). In fig. 22 this compositional field corresponds to a line between X and Y. The original high digenite at locality 3 (fig. 1) has decomposed to various proportions of digenite and chalcocite (Karup-Møller, 1978). This roughly suggests that the chemical composition of the original digenite could have lain on that part of the line X–Y covered by areas B2, B3 and D in fig. 22.

Pure chalcocite occurs alone in silicate minerals and as idiomorphic crystals enclosed in cuprostibite. If the temperatures of formation were below 435°C, then the sulphur fugacity conditions for the sulphide might have corresponded to area B1 and to area E above the cubic Cu_2S–Cu line in fig. 22. However, if the temperatures were above 435° C, then the sulphur fugacity conditions for the pure chalcocite (free of exsolved digenite) would have corresponded to those on or very slightly above the line cubic Cu_2S–Cu.

Cu-Sb-S subtype (II B). The ore mineral associations of this subtype known from localities 2b and 4 in fig. 1 are: (1) skinnerite-tetrahedrite-native antimony - minor chalcostibite, (2) skinnerite-chalcostibite-tetrahedrite and (3) native antimony-tetrahedrite. Sb-oxides are contained in all three associations (Karup-Møller, 1974). They have crystallized late presumably due to increasing fO_2 which gradually stopped the crystallization of the native antimony.

Small amounts of Ag are contained in several of the ore minerals and there is also Fe in one of the two tetrahedrite varieties at locality 4 in fig. 1. The stability lines in fig. 22 are based on pure Cu-Sb minerals. The estimated sulphur fugacity range between 350° and 450°C covering this subtype is shown as area B3 in fig. 22.

The skinnerite–tetrahedrite line, estimated with low accuracy (Craig & Barton,

1973), is positioned in fig. 22 considerably above the stibnite–Sb line. The close association of skinnerite and tetrahedrite with native Sb at locality 2b in fig. 1 and the absence of stibnite suggest that the line should lie below the stibnite–Sb line.

Galena crystallized early in this subtype and was partly replaced by associated Sb-Cu minerals. The non-existence of bournonite places the initial $\log a_{S2}$ values below the bournonite – Cu_2S + PbS + Sb line. At 400°C the $\log a_{S2}$ value would thus be lower than $\sim$–10.9.

The lines for chalcostibite – skinnerite + Sb (no. 3 in fig. 22) and skinnerite – Cu_2S + Sb (no. 4) are below the stibnite – Sb line but above the bournonite – Cu_2S + PbS + Sb line. Stibnite is non-existent in the subtype. The general crystallization sequence was PbS→Sb→Sb-Cu sulphides and oxides. The sulphur fugacity must therefore have increased as the crystallization progressed before crystallization of the Sb-oxides took the place of the native antimony. Until this stage the maximum $\log a_{S2}$ value at 400°C $\sim$–9.2.

At oxygen fugacities between $\log f_{O2}$ $\sim$–23 and $\sim$–31 (327°C), Sb_2O_3 replaces Sb and Sb_2S_3, while both Cu and Cu_2S are not yet oxidized (cf. Holland, 1959, figs 24B and 30). Cu-Sb sulphides may therefore be stable within limited areas of this oxygen fugacity range at sulphur fugacities above and below the Sb–Sb_2S_3 line in fig. 22. Consequently, during the penecontemporaneous crystallization of the Sb-oxides and Sb-Cu sulphides of the Ilímaussaq intrusion (locality 2B and 4 in fig. 1) the prevailing sulphur fugacity could very well have reached above the stibnite–Sb line in fig. 22.

In conclusion, only the pyritization processes within some of the major rocks definitely fall in the region of 'normal ore forming environments' (outlined in figs 21 and 22). The high digenite, the Cu-Sb-S subtype (IIb) and the augite syenite pyrrhotite-chalcopyrite association overlap the 'low sulphur fugacity region' of normal sulphide-forming environments. However, the bulk of the ore minerals from the Ilímaussaq intrusion, for which it is possible to estimate the $\log a_{S2}$ values, distinctly lie below this region.

Oxygen fugacity

Low oxygen fugacity prevailed during the crystallization of the ore minerals in the Ilímaussaq intrusion; this may be due to the high contents of acid volatiles dissolved in the alkaline magma (Kogarko, 1974). A low oxygen fugacity also explains the presence of hydrocarbons in the rocks of the intrusion (Petersilie & Sørensen, 1970; Kogarko, 1974). According to Bailey (1969) and Kogarko (1972) the oxygen fugacity in a crystallizing agpaitic magma is slightly lower than that of the quartz-fayalite-magnetite buffer. Their results were confirmed by Larsen (1976).

The significance of the oxygen and sulphur fugacities for the formation of natural ore mineral parageneses has been studied by Holland (1959), Krauskopf (1965) and others. On the basis of the available thermodynamic data, Holland constructed

the stability fields at 400°, 600°, 800° and 1000°T (Kelvin) for 19 metals, their sulphides and their sulphates as a function of O_2 and S_2 fugacities. The CO_2 fugacity is considered for a few of the metals. Carbonates are extremely rare in the Ilímaussaq intrusion and the influence of CO_2 may therefore be ignored. The fugacity for HCl was not taken into account by Holland (1959). The high content of Cl contained in the Ilímaussaq rocks would suggest the existence of significant HCl fugacities, but even qualitative estimates have not yet been made.

The following phase systems at 327°C (600°K) and 527°C published by Holland (1959) have been used for estimating the oxygen fugacities at which the ore minerals of the Ilímaussaq intrusion crystallized: Fe–O–S, Pb–O–S, Ag–O–S, Cu–O–S and Sb–O–S. The relevant data presented in what follows have been read directly from the diagrams published by Holland (1959). The possible influence on the stability fields of other components, e.g. Cl, has been ignored. The ore minerals in the major rocks are considered before those in the pegmatites and pneumatolytic-hydrothermal veins.

Accessory rock-forming ore minerals

Primary Fe and Ti oxides have not been found by the author in the naujaites, the kakortokites and the lujavrites. Titanomagnetite in rocks belonging to the pulaskite-naujaite series has been described by Larsen (1976). Small amounts of 'droplet' shaped aggregates, representing a high temperature Fe-Ti oxide have crystallized in the sodalite foyaite (fig. 20). Relatively large amounts of a similar phase formed in the augite syenite. In the alkali granite abundant ilmenite and some magnetite crystallized.

The distribution of the Fe-Ti oxides in the Ilímaussaq intrusion thus suggests a distinct decrease in the oxygen fugacity as the crystallization of the Ilímaussaq intrusion progressed from the augite syenite towards the agpaitic nepheline syenites.

Fe–O–S system. The great abundance of magnetite and ilmenite in the alkali granite and the large amounts of the decomposed high temperature Fe-Ti oxide in the augite syenite suggest oxygen fugacities comparable to those prevailing during the consolidation of related magmatic rocks elsewhere. At 527°C magnetite is stable at oxygen pressures ($\log f_{O_2}$ values) between ~–28 (Fe $\leftrightarrow$ Fe_3O_4) and ~–18 (Fe_3O_4 $\leftrightarrow$ Fe_2O_3).

The formation in the white and red kakortokite of the hypogene secondary magnetite-pyrite and magnetite-hematite-pyrite aggregates (figs 10 and 15) suggests that during some presumably late, short-lived moments in the crystallization of these rocks a considerable increase in both the sulphur and the oxygen fugacity took place.

Pb–O–S system. Galena is a common accessory ore mineral in most of the major Ilímaussaq rock types. Native lead is associated with PbS in the lujavrite MC and

may have crystallized as a liquid phase, e.g. at temperatures around 327°C. At this temperature Pb and PbS are oxidized at $\log f_{O2}$ ~-28 and ~-27 respectively. At 527°C the corresponding values are ~-18 and ~-17.

Ore minerals in pegmatites and veins

Pb–O–S system. Galena is a common accessory ore mineral in the pegmatites and pneumatolytic-hydrothermal veins. Native lead is known at one pegmatite locality (locality 5 in fig. 1). The oxidation values for the two minerals are given above.

Sb–O–S system. At localities 2b and 4 (fig. 1) the crystallization of native antimony was gradually followed by the formation of Sb oxides (valentinite and senarmontite) which also replaced the earlier formed Sb (Karup-Møller, 1974). Thus, as the crystallization progressed a gradual increase in the oxygen fugacity took place. At 327°C the Sb is oxidized to Sb_2O_3 at $\log f_{O2}$ ~-31 and at 527°C ~-21.

Cu–O–S system. Primary cuprite is enclosed in antimonian silver at locality 3 (Karup-Møller, 1978) and extremely sparse native copper in dyscrasite at locality 2a. The formation of native copper instead of cuprite suggests $\log f_{O2}$ values rarely dropping below ~-18 (527°C) and ~-22 (327°C).

Ag–O–S system. Silver oxides are not stable in the diagram published by Holland (1959). Ag is replaced by Ag_2SO_4 at $\log f_{O2}$ ~-20 (327°C) and at ~-16 (527°C). The change in these values due to Sb dissolved in antimonian silver (and the fugacity conditions for allargentum and dyscrasite) remains unknown.

The ore minerals in the rocks of the Ilímaussaq intrusion and therefore also the rocks themselves have thus crystallized at a range in oxygen fugacity from $\log f_{O2}$ at more than ~-28 to above ~-18 at temperatures of 527°C. The ore mineral parageneses in pegmatites and pneumatolytic-hydrothermal veins suggest a range in $\log f_{O2}$ from less than ~-31 to ~-20 at 327°C and less than ~-21 to ~-16 at 527°C.

CONCLUSIONS

The bulk of the ore minerals in the rocks, pegmatites and pneumatolytic-hydrothermal veins of the Ilímaussaq crystallized under the low sulphur and oxygen fugacities which are characteristic of agpaitic magmas. Sulphur and oxygen fugacities similar to the low levels of the Ilímaussaq magma have only been recognized at a few terrestrial ore localities. The low sulphur and oxygen fugacities resulted in the formation of native elements, alloys, sulphur-poor sulphides, arsenides and only occasional normal sulphides. Several new mineral species have been described: cuprostibite, skinnerite, chalcothallite and rohaite. Pure westerveldite (FeAs) and seinäjokite ($FeSb_2$) are only known from the Ilímaussaq intrusion. The

unusual mineral djerfisherite is known from chondritic meteorites and from a few terrestrial localities.

Geologically, the Lovozero massif in the USSR resembles the Ilímaussaq intrusion. However, according to Semenov (1972) only a few ore minerals are known from Lovozero: galena, sphalerite, chalcocite, molybdenite, loellingite, safflorite, pyrrhotite (composition apparently not determined), marcasite, pyrite, chalcopyrite and arsenopyrite. The last-named four minerals and possibly also the pyrrhotite suggest oxygen and sulphur fugacity conditions comparable to those of normal ore mineral forming environments.

The crystallization of djerfisherite in pegmatites from the Khibina massif on the Kola penninsula in the USSR suggests low sulphur fugacities, comparable to those at Ilímaussaq.

The accessory ore minerals in the agpaitic rocks of the Ilímaussaq intrusion crystallized late in relation to the host silicate minerals. The sulphides in the augite syenite crystallized early from a liquid immiscibility phase.

According to Ussing (1912) and others the agpaitic stage in Ilímaussaq began with the development of the sodalite foyaite. This is supported by the following ore mineralogical observations:

(1) The mineral pair pyrrhotite-chalcopyrite occurs in the augite syenite and the pair troilite-djerfisherite in the sodalite foyaite, the naujaite and the kakortokites.

(2) Fe-Ti oxides are common in the augite syenite, rare in the sodalite foyaite and absent from the other agpaitic nepheline syenites.

(3) In the augite syenite pyrrhotite has crystallized from an early separated immiscible sulphide phase. In the nepheline syenite it appears to have crystallized relatively late together with the bulk of the other minerals and without any evidence for the existence of an immiscible phase.

The only ore minerals identified in the alkali granite are abundant primary monomineralic magnetite and ilmenite slightly replaced by secondary hematite. Sulphides are entirely absent. The sulphur content in the alkali granite is exceptionally low (~300 ppm) when compared to all the other Ilímaussaq rocks (Gerasimovsky, 1969). Both Ussing (1912) and Ferguson (1970) consider the alkali granite to pre-date the agpaitic rocks. Observations at different localities suggest a mixed origin for the alkali granite. The ore mineralogy observations apparently exclude the alkali granite from being a close relative of the agpaitic rock types.

Acknowledgements

REFERENCES

Bailey, D.K. 1969: The stability of acmite in the presence of H_2O. *Amer. J. Sci.* **267A,** 1-18.

Barton, P. B. 1969: Thermochemical study of the system Fe–As–S. *Geochim. cosmochim. Acta* **33,** 841-857.

Barton, P.B. 1971: The Fe–Sb–S system. *Econ. Geol.* **66,** 121-132.

Barton, P. B. 1973: Solid solutions in system Cu–Fe–S. I. The Cu–S and Cu–Fe–S join. *Econ. Geol.* **68,** 455-465.

Barton, P. B. & Skinner, B. J. 1967: Sulphide mineral stabilities. *In* Barnes H. L. (edit.) *Geochemistry of hydrothermal ore deposits.* 236-333. New York: Hold, Reinhart & Winston.

Blaxland, A. B., Van Breemen, O. & Steenfelt, A. 1976: Age and origin of agpaitic magmatism at Ilímaussaq, south Greenland: Rb-Sr study. *Lithos* **9,** 31–38.

Bohse, H., Brooks, C. K. & Kunzendorf, H. 1971: Field observations on the kakortokites of the Ilímaussaq intrusion, South Greenland, including mapping and analyses by portable X-ray fluorescence equipment for zirconium and niobium. *Rapp. Grønlands geol. Unders.* **38,** 43pp.

Bridgwater, D. & Harry, W. T. 1968: Anorthosite xenoliths and plagioclase megacrysts in Precambrian intrusions of South Greenland. *Bull. Grønlands geol. Unders.* **77** (also *Meddr Grønland* **185,**2) 243 pp.

Craig, J. R. & Barton, D. B. 1973: Thermochemical approximations for sulfosalts. *Econ. Geol.* **68,** 493-506.

Craig, J. R. & Scott, S. D. 1974: Sulphide phase equilibria. *In* Ribbe, P. H. (edit.) *Sulphide mineralogy - short course notes.* CS-1 - CS110. Mineralogical Society of America.

Emeleus, C. H. & Upton, B. G. J. 1976: The Gardar period in South Greenland. *In* Escher, A. & Watt, W. S. (edit.) *Geology of Greenland,* 153–181. Copenhagen: Geological Survey of Greenland.

Engell, J. 1973: A closed system crystal-fractionation model for the agpaitic Ilímaussaq intrusion, South Greenland with special reference to the lujavrites. *Bull. geol. Soc. Denmark* **22,** 334-362.

Engell, J., Hansen, J., Jensen, M., Kunzendorf, H. & Løvborg, L. 1971: Beryllium mineralization in the Ilímaussaq intrusion, South Greenland with description of a field beryllometer and chemical methods. *Rapp. Grønlands geol. Unders.* **33,** 40 pp.

Ferguson, J. 1964: Geology of the Ilímaussaq alkaline intrusion, South Greenland. *Bull. Grønlands geol. Unders.* **39** (also *Meddr Grønland* **172,**4) 81 pp.

Ferguson, J. 1970: The significance of the kakortokite in the evolution of the Ilímaussaq intrusion, South Greenland. *Bull. Grønlands geol. Unders.* **89** (also *Meddr Grønland* **190,**1) 193 pp.

Fuchs, L. H. 1966: Djerfisherite, alkali copper-iron sulphide: A new mineral from enstatite chondrites. *Science, N. Y.* **153,** 166-167.

Genkin, A. D., Troneva, N. V. & Zhuzovlev, N. N. 1969: [First find of the sulphide of potassium, iron and copper - djerfisherite - in ores.] *Geologiya Rudnukh Mestorozhdeniy* **11**(5), 57-64. (In Russian).

Gerasimovsky, V. I. 1969: [*Geochemistry of the Ilímaussaq alkaline massif.*] Moscow: Nauka, 174 pp. (In Russian).

Hamilton, E. I. 1964: The geochemistry of the northern part of the Ilímaussaq intrusion, S. W. Greenland. *Bull. Grønlands geol. Unders.* **42** (also *Meddr Grønland* **162,**10) 104 pp.

Hansen, M. & Anderko, K. 1958: *Constitution of binary alloys.* New York: McGraw-Hill. 1305 pp.

Holland, H. D. 1959: Some applications of thermochemical data to problems of ore deposits. I. Stability relations among the oxides, sulphides, sulphates and carbonates of ore and gangue metals. *Econ. Geol.* **54,** 184-233.

Karup-Møller, S. 1974: Mineralogy of two copper-antimony-sulphide-oxide occurrences from the Ilímaussaq alkaline intrusion in South Greenland. *Neues Jb. Miner. Abh.* **122,** 291-313.

Karup-Møller, S. 1975: On the occurrence of the native lead, litharge, hydrocerussite and plattenerite within the Ilímaussaq alkaline intrusion in South Greenland. *Neues. Jb. Miner. Mh.* **5,** 229-241.

Karup-Møller, S. 1978: Primary and secondary ore minerals associated with cuprostibite. *Bull. Grøn-lands geol. Unders.* **126**, 23-47.

Karup-Møller, S. & Makovicky, E. 1974: Skinnerite, Cu_3SbS_3 - a new copper-antimony sulphosalt mineral. *Amer. Miner.* **59**, 889-895.

Karup-Møller, S. & Makovicky, E. 1977: Westerveldite from the Ilímaussaq alkaline intrusion in South Greenland. Mineralogy, crystallography, mineral associations and conditions of formation. *Neues Jb. Miner. Abh.* **130**, 208-242.

Karup-Møller, S., Løkkegaard, L., Semenov, E. I. & Sørensen, H. 1978: The occurrence of cuprostibite. *Bull. Grønlands geol. Unders.* **126**, 7-22.

Kogarko, L. N. 1972: The role of the compounds of oxygen, sulphur and carbon in magmatic gas phase of alkaline rocks. *Int. geol. Congr. Canada* **10**, 20-24.

Kogarko, L. N. 1974: Role of volatiles. *In* H. Sørensen (edit.) *The alkaline rocks.* 474-488. London: Wiley.

Kogarko, L. N., Ryabchikov, I. D. & Sørensen, H. 1974: Liquid fractionation. *In* Sørensen, H. (edit.) *The alkaline rocks.* 488-500. London: Wiley.

Krauskopf. K. B. (1965): The use of thermochemical data in defining conditions of high-temperature ore formation. *Symp. Problems of Postmagmatic Ore Deposition.* Prague. **2**, 332-355.

Larsen, L. M. 1976: Clinopyroxenes and coexisting mafic minerals from the alkaline Ilímaussaq intrusion, South Greenland. *J. Petrol.* **17**, 258–290.

López-Soler, A., Bosch-Figueroa, J. M., Karup-Møller, S., Besterio, J. & Font-Altaba, M. 1975: Optical study of cuprostibite (Cu_2Sb). *Fortschr. Miner.* **52**, 557-565.

Metcalf-Johansen, J. 1977: Willemite from the Ilímaussaq alkaline intrusion. *Mineralog. Mag.* **41**, 71-75.

Morimoto, N., Gyobu, A., Tsukuma, K. & Koto, K. 1975: Superstructure and nonstoichiometry of intermediate pyrrhotite. *Amer. Miner.* **60**, 240-248.

Mozgova, N.N., Borodaev, Yu.S., Ozerova, N. A., Paakkonen, V., Sveshnikova, O.L., Balitskyi, V. S. & Dorogovin, B. A. 1976: [Seinäjokite ($Fe_{0.8}Ni_{0.2}$) ($Sb_{1.7}As_{0.3}$) and antimonian westerveldite $Fe(As_{0.95}Sb_{0.05})$ from Seinäjoki, Finland.] *Zap. Vses. Miner. Obshch.* **105**, 617-630. (In Russian).

Oen, I. S. & Sørensen, H. 1964: The occurrence of nickel-arsenides and nickel-antimonide at Igdlúnguaq in the Ilímaussaq alkaline massif, South Greenland. *Bull. Grønlands geol. Unders.* **43** (also *Meddr Grønland* **172**, 1) 50 pp.

Oen, I.S. Burke, E. A. J. & Kieft, C. 1977: Westerveldite from Igdlúnguaq, Ilímaussaq alkaline massif, South Greenland. *Mineralog. Mag.* **41**, 77-83.

Petersilie, I. A. & Sørensen, H. 1970: Hydrocarbon gases and bituminous substances in rocks from the Ilímaussaq alkaline intrusion, South Greenland. *Lithos*, **3**, 59-76.

Petruk, W., Cabri, L. J., Harris, D. C., Stewart, J. M. & Clarck, L. A. 1970: Allargentum redefined. *Can. Miner.* **10**, 163-172.

Petruk, W., Harris, D. C., Cabri, L. J. & Stewart, J. M. 1971: Characteristics of the silver-antimony minerals. *Can. Miner.* **11**, 187-195.

Piotrowski, J. M. & Edgar, A. D. 1970: Melting relations of undersaturated alkaline rocks from South Greenland. *Meddr Grønland* **181**, 9, 62 pp.

Ramdohr, P. 1963: The opaque minerals in stony meteorites. *J. geophys. Res.* **68**, 2011-2036.

Roseboom, E. H. 1966: An investigation of the system Cu–S and some natural copper sulphides between 25° and 700° C. *Econ. Geol.* **61**, 641-672.

Rosenqvist, T. 1954: Magnetic and crystallographic studies on the higher antimonides of iron, cobalt and nickel. *Acta Cryst.* **7**, 636.

Semenov: E. I. 1972: [*Mineralogy of the Lovozero alkaline massif.*] Moscow: Akad. Nauk. SSSR. Inst. Mineral. Geokhim. Kristallokhim. Redkikh Elem. (In Russian). 307 pp.

Semenov, E. I., Gerasimovsky, V. I., Maksimova, N. V., Andersen, S. & Petersen, O. V. 1965: Sorensenite, a new sodium-beryllium-tin-silicate from the Ilímaussaq intrusion, South Greenland. *Meddr Grønland* **181**,1, 19 pp.

Semenov, E. I., Sørensen, H., Bessmertnaja, M. S. & Novorossova, L. E. 1967: Chalcothallite - a new sulphide of copper and thallium from the Ilímaussaq alkaline intrusion. South Greenland. *Bull. Grønlands geol. Unders.* **68** (also *Meddr Grønland* **181**,5) 15-26.

Skinner, B. J., Luce, F. D. & Makovicky, E. 1972: Studies of the sulfosalts of copper III : phases and phase relations in the system Cu-Sb-S. *Econ. Geol.* **67**, 924-938.

Sokolova, M. N., Dobrovolskya, M. G., Organova, N. I. & Kuzoxkova, M. E. 1971:[About the find and distribution of djerfisherite in the pegmatites of the Khibina massif.] *Geologiya Rydnykh Mesgtorozhdeniy* **11**, 5, 57-64. (In Russian).

Somanchi, S. 1966: Subsolidus phase relations in the system Ag-Sb. *Can. J. Earth Sci.* **3**, 211-272.

Sørensen, H. 1958: The Ilímaussaq batholith. A review and discussion. *Bull. Grønlands geol. Unders.* **19** (also *Meddr Grønland* **162**,3) 48 pp.

Sørensen, H. 1962: On the occurrence of steenstrupine in the Ilímaussaq massif, Southwest Greenland. *Bull. Grønlands geol. Unders.* **32** (also *Meddr Grønland* **167**,1) 251 pp.

Sørensen, H. 1967: On the history of exploration of the Ilímaussaq alkaline intrusion, South Greenland. *Bull. Grønlands geol. Unders.* **68** (also *Meddr Grønland* **181**,4) 33 pp.

Sørensen, H. 1969: Rythmic igneous layering in peralkaline intrusions. *Lithos* **2**, 261-283.

Sørensen, H. 1970: Internal structures and geological setting of the three agpaitic intrusions - Khibina and Lovozero of the Kola Peninsula and Ilímaussaq, South Greenland. *Can. Miner.* **10**, 299-334.

Sørensen, H., Hansen, J. & Bondesen, E. 1969a: Preliminary account of the geology of the Kvanefjeld area of the Ilímaussaq intrusion, South Greenland. *Rapp. Grønlands geol. Unders.* **18**, 40 pp.

Sørensen, H., Semenov, E. I., Bessmertnaja, M. S. & Khalozovo, E. B. 1969b: [Cuprostibite - a new natural compound of Cu and Sb.] *Zap. Vses Miner. Obshch.* (2), **98**,6, 719–724. (In Russian).

Springer, G. 1967: Die Berechnung von Korrekturen für die quantitative Elektronenstrahl-Mikroanalyse. *Fortsch. Miner.* **45**, 103-124.

Strunz, H. 1970: *Mineralogische Tabellen.* Leipzig: Akademische Verlagsgesellschaft. 621 pp.

Upton, B. G. J. 1974: The alkaline province in South Greenland. *In* Sørensen, H. (edit.) *The alkaline rocks.* 211-228. London: Wiley.

Ussing, N. V. 1912: Geology of the country around Julianehaab. *Meddr Grønland* **38**, 376 pp.

Van Breemen, O. & Upton, B. G. J. 1972: The age of some Gardar intrusive complexes, South Greenland. *Bull. geol. Soc. Amer.* **83**, 3381-3390.